

## Establishing reverse chimeric antigen receptor T cells for precise targeting of immune-mediated thrombotic thrombocytopenic purpura

by Rutuja S Gupte, Sara Rovira Puig, Liliana R. Loureiro, Margot Dierickx, Alexandra von Jutrzenka-Trzebiatowski, Michael Bachmann, Jan Voorberg, Karen Vanhoorelbeke, Claudia Arndt and Anja Feldmann

Received: January 12, 2026.

Accepted: April 7, 2026.

Citation: Rutuja S Gupte, Sara Rovira Puig, Liliana R. Loureiro, Margot Dierickx, Alexandra von Jutrzenka-Trzebiatowski, Michael Bachmann, Jan Voorberg, Karen Vanhoorelbeke, Claudia Arndt and Anja Feldmann. Establishing reverse chimeric antigen receptor T cells for precise targeting of immune-mediated thrombotic thrombocytopenic purpura.

Haematologica. 2026 Apr 16. doi: 10.3324/haematol.2026.300520 [Epub ahead of print]

### *Publisher's Disclaimer.*

*E-publishing ahead of print is increasingly important for the rapid dissemination of science.*

*Haematologica is, therefore, E-publishing PDF files of an early version of manuscripts that have completed a regular peer review and have been accepted for publication.*

*E-publishing of this PDF file has been approved by the authors.*

*After having E-published Ahead of Print, manuscripts will then undergo technical and English editing, typesetting, proof correction and be presented for the authors' final approval; the final version of the manuscript will then appear in a regular issue of the journal.*

*All legal disclaimers that apply to the journal also pertain to this production process.*

## **Establishing reverse chimeric antigen receptor T cells for precise targeting of immune-mediated thrombotic thrombocytopenic purpura**

Rutuja S. Gupte<sup>1</sup>, Sara Rovira Puig<sup>2</sup>, Liliana R. Loureiro<sup>1</sup>, Margot Dierickx<sup>3</sup>, Alexandra von Jutrzenka-Trzebiatowski<sup>1</sup>, Michael Bachmann<sup>1,4,5</sup>, Jan Voorberg<sup>3</sup>, Karen Vanhoorelbeke<sup>2</sup>, #Claudia Arndt<sup>1,6</sup>, #Anja Feldmann<sup>1,4,5</sup>

<sup>1</sup> Department of Radioimmunology, Institute of Radiopharmaceutical Cancer Research, Helmholtz-Zentrum Dresden-Rossendorf, Dresden, Germany

<sup>2</sup> Laboratory for Thrombosis Research, KU Leuven Campus Kulak Kortrijk, Kortrijk, Belgium

<sup>3</sup> Department of Molecular Hematology, Sanquin Research and Landsteiner Laboratory, Amsterdam, The Netherlands

<sup>4</sup> German Cancer Consortium (DKTK), partner site Dresden and German Cancer Research Centre (DKFZ), Heidelberg, Germany

<sup>5</sup> National Center for Tumor Diseases Dresden, Germany; German Cancer Research Center (DKFZ), Heidelberg, Germany; University Hospital Carl Gustav Carus, TUD Dresden University of Technology, Dresden, Germany; Helmholtz-Zentrum Dresden-Rossendorf (HZDR), Dresden, Germany

<sup>6</sup> Mildred Scheel Early Career Center, Faculty of Medicine Carl Gustav Carus, TUD Dresden University of Technology, Germany

#These authors contributed equally

### **Correspondence:**

Name: Dr. Anja Feldmann

Phone number: +49 351 458 3428

Email: [a.feldmann@hzdr.de](mailto:a.feldmann@hzdr.de)

Name: Dr. Claudia Arndt

Phone number: +49 351 458 4049

Email: [c.arndt@hzdr.de](mailto:c.arndt@hzdr.de)

### **Running title:**

Controllable Adapter RevCAR-Ts for iTTP

**Key words:** thrombotic thrombocytopenic purpura; RevCAR T cell; adoptive cell therapy; ADAMTS-13; immunotherapy

**Acknowledgements:**

We would like to thank the students Eugenia Crespo, Haidy A. Saleh Hassan, Karla Elizabeth Gonzalez Soto, Tabea Bartsch, Katharina Hoellen, Fabienne I. Weinberg, Lamice Shurafa, Hugo Boutier, and Nathalia Jones Cifuentes for their precious help. We warmly acknowledge Annegret Riedel, Kim Weiße, Inge Pareyn, Anne-Sophie Delmote and Paul Kaijen for their excellent technical work and support. We also thank Dr. Jurie Tashkandi, Tim Postmus, and PhD. Zsolt Szeles for their valuable inputs. We also thank Torsten Tonn (German Red Cross Blood Donation Service North East, Dresden, Germany) for providing the buffy coats of healthy donors.

**Author contributions:**

Rutuja Gupte: Methodology, Data curation, Validation, Formal Analysis, Visualization, Writing – Original Draft; Sara Rovira Puig: Resources, Writing – Reviewing and Editing; Liliana R. Loureiro: Formal Analysis, Resources, Writing – Reviewing and Editing; Margot Dierickx: Resources, Writing – Reviewing and Editing; Alexandra von Jutrzenka-Trzebiatowski: Resources, Writing – Reviewing and Editing; Michael Bachmann: Supervision, Funding Acquisition, Resources, Writing – Reviewing and Editing; Jan Voorberg: Funding Acquisition, Resources, Writing – Reviewing and Editing; Karen Vanhoorelbeke: Supervision, Funding Acquisition, Resources, Writing – Reviewing and Editing; Claudia Arndt: Conceptualization, Methodology, Formal Analysis, Supervision, Funding Acquisition, Project Administration, Resources, Writing – Original Draft; Anja Feldmann: Conceptualization, Methodology, Supervision, Funding Acquisition, Project Administration, Resources, Writing – Reviewing and Editing

**Funding:** This work was supported by funds of the EU MSCA project TOLERATE by the European Union under Grant Agreement No. 101072729 and funded by the European Union under Grant Agreement No. 101115159 (Horizon EIC 2022 Pathfinder challenges 01 project B-specific). Views and opinions expressed are however those of the author(s) only and do not necessarily reflect those of the European Union or European Research Executive Agency or the European Innovation Council and SMEs Executive Agency (EISMEA). Neither the European Union nor the granting authority can be held responsible for them.

**Conflict of interest disclosure:** M.B. has filed patents related to the RevCAR system and the anti-La mAbs.

**Data-sharing statement:**

Data for this manuscript is available on request from the corresponding author.



## **Abstract:**

Immune-mediated Thrombotic Thrombocytopenic Purpura (iTTP) is a life-threatening autoimmune disorder caused by autoantibodies that target the metalloprotease ADAMTS13. This prevents the cleavage of Ultra-Large von Willebrand Factor (UL-VWF), thereby forming microthrombi in the microvasculature. While current treatments are effective, ADAMTS13 relapses occur in up to 15% of the patients after rituximab administration. In this study, we propose a novel approach addressing the unmet need for treatment of patients with ADAMTS13 refractoriness and for patients requiring repeated treatment. Our strategy involves developing two targeted therapies that aim to achieve highly effective and safe B cell depletion. For the first time, we employ adapter Chimeric Antigen Receptor (CAR) T cells called Reverse CAR (RevCAR) T cells to (i) achieve a broader and deeper B cell depletion by targeting CD19 and (ii) selectively deplete the disease-causing anti-ADAMTS13 autoreactive B cells to increase precision and safety in iTTP treatment. Therefore, we have developed novel Target Modules (RevTMs) against CD19<sup>+</sup> and anti-ADAMTS13 autoreactive B cells. We show that the RevCAR T cells successfully and specifically kill target hybridomas and Nalm-6 cells in a RevTM-dependent manner and at low effector-to-target cell ratios. Moreover, the RevCAR T cells are able to eliminate the target cells even in the presence of high concentrations of ADAMTS13 autoantibodies. Overall, our findings demonstrate for the first time, a proof-of-concept that anti-ADAMTS13 autoreactive B cells can be selectively depleted by the RevCAR T cell platform paving the way for an effective and safe therapy for iTTP.

## **Introduction:**

Immune-mediated Thrombotic Thrombocytopenic Purpura (iTTP) is a rare and life-threatening autoimmune disease (AID) characterized by thrombotic microangiopathy. The pathophysiology of iTTP is primarily characterized by the presence of autoantibodies against ADAMTS13 (a disintegrin and metalloprotease with thrombospondin type 1 motif, member 13), an enzyme that is important for the proteolytic cleavage of endothelial Ultra-Large von Willebrand Factor (UL-VWF)(1-4). It contains distinct functional domains, namely; metalloprotease (M), disintegrin-like (D), thrombospondin type 1 repeats (T1-T8), a cysteine-rich region (C), spacer (S), and CUB domains (CUB1-CUB2) (3). Autoantibody-induced clearance and/ or inhibition of ADAMTS13 (5) and resultant accumulation of UL-VWF in the microvasculature(6, 7), causes spontaneous formation of microthrombi, microangiopathic hemolytic anemia, and severe thrombocytopenia in iTTP patients. If left untreated, these conditions can ultimately lead to fatal multiorgan failure. The existing standard-of-care therapeutic regimen involving Therapeutic Plasma Exchange, systemic immunosuppression with corticosteroids and B-cell depleting anti-CD20 rituximab, and caplacizumab(8-11), has substantially improved survival and acute disease control. However, these approaches do not selectively eliminate the ADAMTS13-specific autoreactive immune clones. Although many patients achieve durable clinical remission, persistence or recurrence of reduced ADAMTS13 activity is still a risk and necessitates long-term monitoring and, in some cases, repeated immunosuppression. Although exact numbers for refractory patients depend on the population under study, there have been reports of incidence of ADAMTS13 refractoriness still being as high as 12.5 – 17.9%(12). This highlights the need for autoreactive BCR-directed cellular therapies that may potentially reduce the need for ongoing, non-specific immunosuppression following initial intervention.

Targeted immunotherapies, particularly Chimeric Antigen Receptor (CAR) T cells, which are known for their high success rates in treating B cell malignancies(13, 14), have gained much attention in AID.  $\alpha$ -CD19 CAR T cells have shown promising efficiency in depleting autoreactive B cells in AID (15, 16). However, as a pan-B-cell-depleting therapy, they also attack non-pathogenic B cells, causing lifelong B cell aplasia, ultimately compromising humoral immunity. More recently, chimeric autoantigen receptor (CAAR) T cells have been developed to selectively target pathogenic B cells while sparing non-pathogenic ones in various AIDs, such as pemphigus vulgaris, Graves' disease, and N-methyl-D-aspartate receptor encephalitis(17, 18). Nevertheless, all the conventional CA(A)R-T approaches still pose significant risks as they lack direct control mechanisms to rapidly manage side effects, such as cytokine release syndrome (CRS) and neurotoxicity(19).

To facilitate controllability, minimize side effects, and allow for precise targeting of autoreactive B cells in iTTP patients, we here present for the first time a novel switchable adapter CAR system developed based on the Reverse CAR (RevCAR) T cell platform(20-22), which recently entered first clinical trials for treatment of CD123<sup>+</sup> hematological malignancies (NCT05949125). This platform is based on the interaction between the RevCAR on T cells and its corresponding adapter molecule, the Reverse Target Module (RevTM) (Figure 1A). Extracellularly, the RevCAR contains a short peptide epitope (E5B9) derived from the human La protein(23-25) and is fused to intracellular CD28/ CD3 $\zeta$  signaling domains. RevCAR-T cell activity is finely regulated by the RevTM, a tunable bispecific adapter that simultaneously binds to the E5B9 epitope on RevCAR-T cells and a surface entity on target cells. We here employ the RevCAR system to investigate and compare the efficacy of two different retargeting strategies in Nalm-6 and hybridoma cell models. First, we designed a novel CD19-specific

RevTM that allows broader, deeper and temporally controlled pan B-cell depletion. This approach was founded on the established capacity of CD19-directed CAR T cells in achieving effective deep tissue penetration and robust B-cell depletion in malignant settings and other AIDs. Second, to specifically deplete autoreactive B cells in iTTP via the RevCAR system, a set of ADAMTS13-derived RevTMs was developed. This would enable redirection of RevCAR-T cells exclusively against disease-causing polyclonal  $\alpha$ -ADAMTS13 autoreactive B cells. Both strategies have the potential to also be applied in other B-cell-driven AIDs. Moreover, this would help illustrate the flexibility of the system in scenarios where specific or broader B-cell targeting may be clinically indicated even beyond iTTP.

## **Methods**

### **RevCAR T-cell generation**

Human PBMCs were isolated from healthy donor buffy coats (German Red Cross, Dresden) by Pancoll density centrifugation. Pan-T cells were obtained by negative magnetic selection using the Pan T Cell Isolation Kit (Miltenyi Biotec) and cultured for 3 days in RPMI complete medium supplemented with IL-2 (50U/mL). T cells were activated with T-Cell TransAct™ and transduced with lentiviral vectors to generate RevCAR T cells as previously described(21). During transduction, cells were maintained in TexMACS medium (Miltenyi Biotec) supplemented with IL-2, -7, and -15 (Miltenyi Biotec). Prior to experiments, RevCAR T cells were transferred to cytokine-deprived RPMI<sub>complete</sub> medium for 24h.

### **Purification and characterization of RevTMs**

For RevTM purification,  $2 \times 10^6$  RevTM-producing 3T3 cells were seeded in a T175 flask (Greiner Bio-One). On day 4, supernatants were harvested and centrifuged at  $360 \times g$  for 3 min at  $4^\circ\text{C}$ , then  $10,000 \times g$  for 20 min at  $4^\circ\text{C}$ . Cleared supernatants were purified using a Strep-Tactin®XT 4Flow® column (IBA-Lifesciences) according to the manufacturer's instructions. Elution fractions were dialyzed in  $1 \times \text{PBS}$ .

### **Cytotoxicity assay**

To assess RevCAR T-cell cytotoxicity, Nalm-6 or hybridoma cells were labeled with eFluor™ 670 following the manufacturer's protocol. Cells were washed with ice-cold PBS, stained for 15 min at  $37^\circ\text{C}$ , quenched with cold medium, and washed to remove excess dye. Labeled target cells ( $2 \times 10^4$ ) were co-cultured with RevCAR T cells  $\pm$  RevTMs in 96-well plates (200 $\mu\text{L}$ ). Target cells alone served as a minimum control. Unless specified, the E:T ratio was 2.5:1 and the RevTMs were used at saturating concentrations of 25nM for CUB and MDTCS RevTMs; and 5nM for fL and  $\alpha$ -CD19 RevTMs. After incubation, 20 $\mu\text{L}$  was diluted 1:5 in DAPI solution and eFluor™ 670<sup>+</sup> cells were quantified using a MACSQuant VYB Analyzer. The following equation was used to calculate the % lysis of target cells:

$$\% \text{ Lysis} = \frac{(\text{Minimum killing} - \text{Specific killing})}{\text{Minimum killing}} * 100$$

For autoantibody assays,  $5 \times 10^4$  RevCAR T cells and  $2 \times 10^4$  target cells were co-cultured  $\pm$  25nM CUB or MDTCS RevTM and 1.6–20 $\mu\text{g}/\text{mL}$  autoantibody in a final volume of 200 $\mu\text{L}$ .

## **Cytokine release assay**

Cell-free supernatants of cytotoxicity assays (see above) were collected after 24h to determine the concentration of cytokines released into co-culture supernatants. OptEIA Human interleukin-2 (IL-2), tumor necrosis factor (TNF), interferon gamma (IFN- $\gamma$ ), granulocyte-macrophage colony-stimulating factor (GM-CSF) ELISA kits were used according to the manufacturer's instructions (BD BioSciences). The samples were diluted 1:10 before analysis. Assays were readout using the Infinite M200 pro plate reader and Magellan™ software (TECAN).

## **Intracellular staining**

After 24h co-incubation of  $5 \times 10^4$  RevCAR T cells with  $2 \times 10^4$  target cells  $\pm$  25nM RevTM, RevCAR T cells were harvested and stained for intracellular granzyme B and perforin as previously described(26-28). Briefly, cells were first stained extracellularly with  $\alpha$ -human CD8 PE-Vio770 (Miltenyi Biotec) and Zombie Red™ (BioLegend), then fixed and permeabilized using the Inside Stain kit (Miltenyi Biotec) according to manufacturer instructions. During permeabilization, 5 $\mu$ L FcR Blocking Reagent was added to prevent nonspecific binding. Cells were then incubated for 30 min with  $\alpha$ -human Granzyme B-PE (1:20) and  $\alpha$ -human Perforin-VioBlue™ (1:10). Data acquisition was performed on a MACSQuant10 Analyzer and analyzed using MACSQuantify and FlowJo™.

## **Ethics statement:**

Ethical approval for research involving human T cells was obtained from the local ethics committee of the Medical Faculty Carl Gustav Carus, Technische Universität Dresden, Germany (EK138042014).

## **Results:**

### **Design of novel RevTMs for flexible and safe targeting of autoreactive B cells in iTTP**

To generate targeted therapy for iTTP with increased safety profile, we developed two distinct adapter CAR approaches based on the RevCAR system(21, 29), by creating RevTMs with distinct specificity.

First, to activate RevCAR T cells for temporally controlled pan-B-cell depletion, an  $\alpha$ -CD19 RevTM was generated by fusing the deimmunized scFv of the  $\alpha$ -CD19 mAb (clone HD37) to the humanized scFv of the  $\alpha$ -La mAb (clone 5B9) via short peptide linkers. Second, a more specific approach was implemented to eliminate only the disease-causing autoreactive B cells. To this end, RevTMs were engineered to contain either the full-length ADAMTS13 autoantigen (fL RevTM) (Figure 1A) or highly immunogenic ADAMTS13 subdomains (MDTCS RevTM and CUB RevTM containing MDTCS or CUB1-2 domains, respectively)(30, 31). Since ADAMTS13 has proteolytic activity, an E225Q mutation was introduced into the M domain (31) to ensure that ADAMTS13 and its fragments within the RevTMs are enzymatically inactive. All RevTMs are endowed with an N-terminal Ig kappa leader and C-terminal purification tags (His, Strep). To produce RevTMs, stable eukaryotic expression cell lines were established using 3T3 fibroblast cells. As shown in Supplementary Figure S1C and S1D, the  $\alpha$ -



CD19 RevTM as well as ADAMTS13 RevTM, MDTCS RevTM and CUB RevTM were successfully purified from cell culture supernatants in sufficient quality and quantity.

### **RevTMs bind successfully to both RevCAR T cells and target cells**

To characterize the novel  $\alpha$ -CD19, fL, MDTCS and CUB RevTMs, we first analyzed their binding properties to both RevCAR T cells and target cells.

As shown in Figure 1B and 1C, human T cells could be successfully transduced with the RevCAR at a high efficiency of ~60%, resulting in an average expression of 5,700 RevCARs per cell. RevTM binding towards RevCAR T cells was assessed using  $\alpha$ -His Phycoerythrin (PE) Ab. Flow cytometric analysis demonstrated comparable binding to EGFP<sup>+</sup> RevCAR T cells for all novel RevTMs (Figure 1D).

To further investigate the binding of the novel RevTMs to  $\alpha$ -ADAMTS13 B cell receptor (BCR)<sup>+</sup> cells and to subsequently test their functional properties, two cell models were chosen: (i) our in-house available hybridoma cell lines that naturally express  $\alpha$ -human ADAMTS13 BCR specific against S (mAb clone 15D1)(32) or CUB domains (mAb clone 20D2)(33) and (ii) the CD19<sup>+</sup> human B cell line Nalm-6, engineered to overexpress patient-derived  $\alpha$ -human ADAMTS13 scFvs on its surface (termed surrogate decoy receptor, SDR) (Supplementary Figures S2A and S2C). SDRs were designed using the scFvs derived from the patient  $\alpha$ -ADAMTS13 mAbs II-1 and z1-201(34-37), that are specific for the S and CUB domains of the ADAMTS13 autoantigen, respectively. To create the  $\alpha$ -ADAMTS13 SDR, the patient-derived scFvs were fused to the CD28 transmembrane domain for anchoring them on the cell surface (Supplementary Figure S2C). Extracellularly, the receptor is equipped with the E7B6 tag for flow cytometric detection. Nalm-6 cells were engineered to stably overexpress the  $\alpha$ -S (Nalm-6  $\alpha$ -S) and  $\alpha$ -CUB SDR (Nalm-6  $\alpha$ -CUB) via lentiviral transduction.

As confirmed by flow cytometry, the majority of both hybridomas and engineered Nalm-6 cells express  $\alpha$ -human ADAMTS13 BCRs and SDRs, respectively, on their surface. The receptor densities range from ~10,000 to ~200,000 molecules per cell (Supplementary Figure S2), which is consistent with the average number of BCRs found on human B cells (15,000 to 100,000) (38, 39).

As summarized in Figure 1E-G, the  $\alpha$ -CD19 RevTM and all ADAMTS13 RevTMs showed specific binding to their respective target cells. In comparison to the MDTCS and CUB RevTM, the fL RevTM demonstrated considerably lower binding, particularly toward hybridoma cells, as indicated by reduced MFI values.

### **RevTMs successfully redirect RevCAR T cells to kill CD19<sup>+</sup> and $\alpha$ -ADAMTS13 BCR/SDR<sup>+</sup> target cells**

Having validated the binding properties of the novel RevTMs, we assessed their cytotoxic potential in the context of the RevCAR system.

First, in order to check the therapeutic window, killing capacity of the different RevCAR systems was evaluated using serial dilutions of RevTMs. Thus, titrating the RevTM concentrations would be useful in determining the redirection capabilities of the RevTMs even at lower concentrations. Briefly, eFluor 670-stained target cells were co-cultured with RevCAR

T cells with or without RevTM for 24 hours. Post-incubation, the number of target cells were enumerated via flow cytometry (Figure 2). As shown in Figure 2A, all RevTMs showed concentration-dependent redirection of RevCAR T cells against Nalm-6 target cell lines. The half-maximal effective concentration ( $EC_{50}$ ) was in the low picomolar range for  $\alpha$ -CD19, MDTCS and CUB RevTMs, and in the low nanomolar range for the fL RevTM. At 5nM all RevTMs were in the saturated plateau phase, showing maximum killing of 60-80% after 24 hours (Figure 2A). Compared to Nalm-6 cell lines, after using hybridomas in co-culture assays,  $EC_{50}$  values obtained were 100- to 10,000-fold higher for CUB and MDTCS RevTMs (Figure 2B). However, no significant killing was observed for fL RevTM (Figure 2C), which might be attributed to its lower binding capability toward hybridomas than toward SDR<sup>+</sup> Nalm-6 cells (Figure 1 E-G).

Second, we also attained information about the RevCAR T cell functionality under different E:T ratios. This is of relevance in secondary lymphoid organs e.g. spleen, where autoreactive B cell numbers are high(40) and RevCAR T cells may be overpowered (Figure 3). All the RevTMs efficiently redirected RevCAR T cells to kill Nalm-6 cells at different E:T ratios (Figure 3A, B). As expected, the  $\alpha$ -CD19 RevTM and fL RevTM effectively engaged RevCAR T cells to kill both the Nalm-6  $\alpha$ -S and the Nalm-6  $\alpha$ -CUB cell lines. In contrast, MDTCS RevTM specifically killed the Nalm-6  $\alpha$ -S line while the CUB RevTM killed the Nalm-6  $\alpha$ -CUB cell line. Even at a limiting E:T ratio of 1:5, the  $\alpha$ -CD19, MDTCS and CUB-based systems achieved a high specific killing of up to 60%, while the fL RevTM achieved similar efficacy only at 1:1 E:T ratio. These findings are consistent with the hybridoma results (Figure 3 C, D). CUB and MDTCS RevTMs were able to efficiently target the  $\alpha$ -CUB and  $\alpha$ -S hybridomas, respectively. Vice versa, when MDTCS and CUB RevTMs were used against target-negative hybridomas, no target cell lysis was observed, thereby underscoring the target specificity of the system (Supplementary Figure S4). However, in line with the results obtained in Figure 2, no killing of  $\alpha$ -CUB and  $\alpha$ -S hybridomas occurred with the fL RevTM (Figure 3 C, D).

### **RevTMs specifically stimulate RevCAR T cells to upregulate and release various effector molecules**

We next assessed the expression of various effector molecules expressed by the CAR T cells representing their activation, proliferative capacity, and cytotoxic potential. In particular, we examined the cytokine profile for Interleukin-2 (IL-2), Tumor Necrosis Factor (TNF), Interferon gamma (IFN- $\gamma$ ), as known immunomodulatory cytokines, and granulocyte-macrophage colony-stimulating factor (GM-CSF) as a stimulator of innate immune components. Additionally, we also assessed perforin, and granzyme B levels as important drivers of cytotoxicity.

For this, we first investigated supernatants from cytotoxicity co-culture assays collected after 24 hours. As shown in Figure 4A-D, RevCAR T cells were stimulated to secrete different pro-inflammatory cytokines (TNF, IFN- $\gamma$ , GM-CSF) and the growth-promoting cytokine IL-2 in the presence of  $\alpha$ -CD19, CUB or MDTCS RevTMs and their respective target hybridoma and Nalm-6 cells (Figure 4 A-D). Upon fL RevTM-mediated redirection of RevCAR T cells against  $\alpha$ -S and  $\alpha$ -CUB Nalm-6 cells, only minimal or no cytokines were detectable in the co-culture supernatant which is in line with their inability to kill the target cells (Figure 2 and 3, Supplementary Figure S3A). Second, redirected RevCAR T cells were analyzed via flow

cytometry for the upregulation of intracellular granzyme B and perforin. The cells were also stained with  $\alpha$ -CD8 antibody to determine potential differences in granzyme B and perforin expression among CD8-positive and CD8-negative cells. Both the pan-B cell depleting  $\alpha$ -CD19 RevTM, and the ADAMTS13-specific RevTMs (CUB, MDTCS, and fL RevTMs) stimulated RevCAR T cells to specifically upregulate granzyme B and perforin. This effect was only observed upon cross-linkage with their corresponding target cell lines (Figure 5, Supplementary Figure S3B). Interestingly, both CD8-positive and CD8-negative RevCAR T cells expressed cytotoxic molecules to a comparable extent, suggesting that TM-dependent RevCAR activation induces the same cytotoxic effector mechanisms in both T cell subtypes, and can also stimulate CD8-negative T cells to exert a cytotoxic function (Figure 5).

### **The presence of autoantibodies does not hamper the cytotoxic potential of the RevCAR system**

iTTP is predominated by the presence of  $\alpha$ -ADAMTS13 autoantibodies in patient plasma. To elucidate whether these circulating autoantibodies interfere with the performance of the RevCAR system, we set-up cytotoxicity assays in the absence or presence of  $\alpha$ -ADAMTS13 Abs that compete with the respective TMs using either II-1/ z1-201 patient-derived antibodies and 15D1/ 20D2 mAbs for Nalm-6 and hybridoma co-cultures, respectively. As described in (41), the  $\alpha$ -ADAMTS13 autoantibody titers were evaluated in a cohort of 48 iTTP patients. This assessment employed both the Technozyme inhibitor ELISA and an in-house ELISA, revealing  $\alpha$ -ADAMTS13 autoantibody titers of up to 590 IU/mL and up to 19.5  $\mu$ g/ mL, respectively. Therefore, we applied a concentration range of 1.5  $\mu$ g/ mL to 20  $\mu$ g/ mL to ensure a suitable high titer of these antibodies(41). As shown in Figure 6, RevCAR T cells redirected by either the MDTCS or the CUB RevTM, achieved approximately 80% killing of Nalm-6 or hybridoma cells expressing either  $\alpha$ -S or  $\alpha$ -CUB SDR/ BCR, respectively within 24 hours. Thus, the addition of competing autoantibodies across all tested conditions did not influence the RevCAR system as they maintained their cytotoxic potential. There was only a slight inhibition observed at the highest Ab concentration of 20 ng/ $\mu$ L, particularly in assays using the hybridomas. On a molecular level, at 20 ng/ $\mu$ L of autoantibody concentration, the molar ratio of RevTM to autoantibody is 1:5. This infers that the cytotoxic potential of the system is hampered only by ~20% even when the antibody molecules are five times more than the RevTMs (Figure 6B). Thus, high concentrations of clinically relevant antibodies do not significantly impair the cytotoxic effects of the RevCAR system.

### **Discussion:**

AID are chronic diseases, in which the immune system attacks the body's own cells leading to tissue, organ damage and even death. Current treatment options, including for iTTP, primarily focus on symptom management, e.g. general immunosuppression, rather than addressing the underlying cause, thereby compromising both cellular and humoral immunity. This is accompanied by relapse and refractoriness(42, 43), for which the treatment is particularly challenging and clinical guidelines are scarce. In iTTP, ADAMTS13 refractoriness has been observed in up to 15% of patients following rituximab administration, and even 60% of patients experience ADAMTS13 relapses, necessitating repeated rituximab administrations over the course of several years in many cases. Therefore, it remains a substantial unmet clinical need for personalized curative treatment strategies(44).

The targeted elimination of the B cell repertoire, encompassing autoreactive B cells, via  $\alpha$ -CD19 CAR T cells, has shown highly encouraging outcomes in patients with ulcerative colitis, severe myositis and systemic sclerosis, as these patients have entered long-term remissions without AID symptoms(45, 46). This development represents a significant advancement, as it provides AID patients with access to potential curative treatments and opens new avenues for their care and management.

In this study, we present for the first time, a controllable adaptor-based RevCAR T cell platform for deep, selective and safe elimination of both pan B cells, as well as of the disease-causing  $\alpha$ -ADAMTS13 autoreactive B cells in iTTP. For this we designed RevTMs against CD19 allowing general B cell depletion, and RevTMs containing parts of or the entire ADAMTS13 protein. Our *in vitro* data confirm the highly potent and sensitive pan ( $\alpha$ -CD19) or ADAMTS13-specific elimination of various target B cell lines via the RevCAR system at low E:T ratios and low RevTM concentrations, for both approaches. Upon cross-linkage with target cells via  $\alpha$ -CD19 or ADAMTS13 RevTMs (MDTCS, CUB), RevCAR T cells further showed marked upregulation of cytotoxic effector molecules like granzyme B and perforin while also releasing various effector cytokines, including TNF, IFN- $\gamma$ , IL-2 and GM-CSF. This underscores that RevCAR T cells are activated in a strict RevTM- and target-dependent manner. Despite its high activity against Nalm-6 cells, the fL RevTM demonstrated reduced binding and cytotoxic activity against the target hybridoma cells. As the underlying cause of this observation was not immediately apparent, we evaluated its conformational state and found that it predominantly adopts an open conformation (data not shown). Since this structural orientation may permit exposure of both cryptic and non-cryptic epitopes of ADAMTS13, thereby enabling engagement of a broader range of autoreactive B-cell clones, the mechanistic basis for the reduced efficacy still remains unclear. Further characterization of the fL RevTM, including e.g. assessment of post-translational modifications will be required to clarify the observed differences. Overall, through a comparative analysis of the various ADAMTS13 RevTMs, we identified MDTCS and CUB RevTMs, encompassing the most immunogenic domains of the ADAMTS13 protein(1, 3), as the lead candidates in terms of their cytotoxic potency, while  $\alpha$ -CD19 RevTM is a promising candidate for a less specific but temporal pan B-cell reset via the RevCAR system.

In contrast to the CD19-specific RevCAR approach, circulating autoantibodies in iTTP patients may clinically hinder the successful application of ADAMTS13-based RevTMs and negatively affect treatment efficacy due to their binding to RevTMs. We have addressed such concerns, and based on the results from the competition assays performed, we consider the risk to be rather low. Our data underline that both MDTCS and CUB RevCAR systems are only moderately hampered in the presence of high concentrations of competing autoantibodies. Even at an autoantibody concentration of 20  $\mu$ g/mL, RevTMs were still found to be highly effective in redirecting RevCAR T cells. According to Pos et al(41), this concentration corresponds to the highest levels of  $\alpha$ -ADAMTS13 autoantibody titers observed in a cohort of 48 iTTP patients. Unlike conventional CA(A)R approaches, where potential drops in treatment efficiency can only be compensated by infusing higher CA(A)R T cell numbers, in the RevCAR system it can be achieved by simply increasing the RevTM dose. Furthermore, the risk to fix complement to RevTM-autoantibody complexes or mediate antibody-dependent cellular cytotoxicity in iTTP is low, as the most predominant isotype in iTTP relapse is IgG4(47-49).

Similar to all adaptor and conventional CAR-T approaches, potential clinical application of the RevCAR platform in AID, including iTTP, would involve transient lymphodepleting

preconditioning to facilitate engraftment and expansion of the infused RevCAR T cells. As known from CD19-directed CAR T-cell therapy, preconditioning has been generally well tolerated in patients with selected autoimmune indications(15). However, additional studies will be necessary to further optimize conditioning regimens and carefully balance benefit-risk ratios. Compared to conventional CARs, a central advantage of the RevCAR system lies in its modular design with its universal RevCAR-T cells and short-lived, switchable adaptor molecules (RevTM) providing an intrinsic safety mechanism. The principle of applying adaptor CAR therapies has been clinically explored in our recent phase I study of the related adaptor platform “UniCAR”(50, 51). After infusing a single dose of CAR T cells, UniCAR T-cell activation can be regulated through controlled administration of the target-specific TMs. Similarly, a clinical application of the RevCAR system in iTTP would involve initial RevCAR-T cell administration followed by continuous RevTM infusion for several weeks during the initial phase. Moreover, in the event of a (ADAMTS13) relapse, therapy could be reinitiated upon repeated RevTM dosing. To facilitate management of acute toxicities of CAR T cells in AIDs, like cytokine release syndrome, as well as long-term consequences such as sustained B-cell aplasia, RevTM administration could be discontinued to immediately terminate RevCAR-mediated signaling. Especially for autoimmune patients who may already have a compromised immune system, its inherent control mechanism represents a significant advantage over conventional CA(A)R approaches. The feasibility of such a rapid and temporal control switch has been successfully proven in the related adaptor CAR approach “UniCAR”(50, 51), where adaptor-dependent UniCAR T cells remained detectable for up to 6 months. They also demonstrated re-expansion upon adaptor re-infusion after treatment-free intervals(50, 51).

In addition, the modular architecture of the RevCAR system permits redirection of the same CAR T-cell product toward multiple targets through exchange of RevTM specificity, thereby expanding therapeutic flexibility. Clinically, the simultaneous or subsequent combination of MDTCS and CUB RevTMs would be a highly promising strategy for treatment of iTTP patients, as they together address the majority of disease-relevant epitopes(1, 3), and thus would enable RevCAR T cells to efficiently eliminate nearly all  $\alpha$ -ADAMTS13 autoreactive B cells in patients. Alternatively, or in case of relapse, the herein presented  $\alpha$ -CD19 RevTM can be used for pan B cell reset via the RevCAR system. While bispecific antibodies can also provide conditional T-cell engagement, these molecules typically rely on CD3-mediated TCR signaling, which may be downregulated upon T-cell activation(52, 53). In contrast, RevCARs provide their own activation and co-stimulatory domains, ensuring sustained functionality across all T cell subtypes.

In conclusion, the present study establishes proof-of-principle for the adaptor RevCAR T-cell platform in iTTP, representing the first application of such a system to selectively target autoreactive B cells in the disease. Thus, it offers iTTP patients a prospective curative treatment option and also poses significant potential for successful application in other AIDs.

## References

1. Joly BS, Coppo P, Veyradier A. Thrombotic thrombocytopenic purpura. *Blood*. 2017;129(21):2836-2846.
2. Zheng XL, Vesely SK, Cataland SR, et al. ISTH guidelines for the diagnosis of thrombotic thrombocytopenic purpura. *J Thromb Haemost*. 2020;18(10):2486-2495.
3. Kremer Hovinga JA, Coppo P, Lammle B, et al. Thrombotic thrombocytopenic purpura. *Nat Rev Dis Primers*. 2017;3:17020.
4. Cataland SR, Coppo P, Scully M, Lammle B. Thrombotic thrombocytopenic purpura: 100 years of research on Moschcowitz syndrome. *Blood*. 2024;144(11):1143-1152.
5. Snyder MR, Maitta RW. Anti-ADAMTS13 autoantibodies in immune-mediated thrombotic thrombocytopenic purpura. *Antibodies (Basel)*. 2025;14(1):24.
6. Tersteeg C, Verhenne S, Roose E, et al. ADAMTS13 and anti-ADAMTS13 autoantibodies in thrombotic thrombocytopenic purpura - current perspectives and new treatment strategies. *Expert Rev Hematol*. 2016;9(2):209-221.
7. Thomas MR, de Groot R, Scully MA, Crawley JT. Pathogenicity of Anti-ADAMTS13 Autoantibodies in Acquired Thrombotic Thrombocytopenic Purpura. *EBioMedicine*. 2015;2(8):942-952.
8. Coppo P, Bubenheim M, Azoulay E, et al. A regimen with caplacizumab, immunosuppression, and plasma exchange prevents unfavorable outcomes in immune-mediated TTP. *Blood*. 2021;137(6):733-742.
9. Reff ME, Carner K, Chambers KS, et al. Depletion of B cells in vivo by a chimeric mouse human monoclonal antibody to CD20. *Blood*. 1994;83(2):435-445.
10. Zheng XL. The standard of care for immune thrombotic thrombocytopenic purpura today. *J Thromb Haemost*. 2021;19(8):1864-1871.
11. Weisinger J, Blanchard F, Suzon B, et al. Ethnicity affects relapse-free survival in immune-mediated thrombotic thrombocytopenic purpura. *Haematologica*. 2026 Jan 8. doi: 10.3324/haematol.2025.288789. [Epub ahead of print]
12. Du P, Cristarella T, Goyer C, Moride Y. A systematic review of the epidemiology and disease burden of congenital and immune-mediated thrombotic thrombocytopenic purpura. *J Blood Med*. 2024;15:363-386.
13. Awasthi R, Maier HJ, Zhang J, Lim S. Kymriah(R) (tisagenlecleucel) - An overview of the clinical development journey of the first approved CAR-T therapy. *Hum Vaccin Immunother*. 2023;19(1):2210046.

14. Weinstein B, Muresan B, Solano S, et al. Efficacy and safety of innovative experimental chimeric antigen receptor (CAR) t-cells versus axicabtagene ciloleucel (Yescarta) for the treatment of relapsed/refractory large b-cell lymphoma (LBCL): matching adjusted indirect comparisons (MAICs) and systematic review. *Innov Pharm.* 2021;12(4):10.24926/iip.v12i4.4345.
15. Muller F, Taubmann J, Bucci L, et al. CD19 CAR T-Cell therapy in autoimmune disease - a case series with follow-up. *N Engl J Med.* 2024;390(8):687-700.
16. Haghikia A, Hegelmaier T, Wolleschak D, et al. Anti-CD19 CAR T cells for refractory myasthenia gravis. *Lancet Neurol.* 2023;22(12):1104-1105.
17. Ellebrecht CT, Bhoj VG, Nace A, et al. Reengineering chimeric antigen receptor T cells for targeted therapy of autoimmune disease. *Science.* 2016;353(6295):179-184.
18. Reincke SM, von Wardenburg N, Homeyer MA, et al. Chimeric autoantibody receptor T cells deplete NMDA receptor-specific B cells. *Cell.* 2023;186(23):5084-5097.e18.
19. Adkins S. CAR T-Cell Therapy: Adverse events and management. *J Adv Pract Oncol.* 2019;10(Suppl 3):21-28.
20. Crespo E, Loureiro LR, Stammberger A, et al. RevCAR-mediated T-cell response against PD-L1-expressing cells turns suppression into activation. *NPJ Precis Oncol.* 2025;9(1):42.
21. Feldmann A, Hoffmann A, Bergmann R, et al. Versatile chimeric antigen receptor platform for controllable and combinatorial T cell therapy. *Oncoimmunology.* 2020;9(1):1785608.
22. Saleh HA, Mitwasi N, Ullrich M, et al. Specific and safe targeting of glioblastoma using switchable and logic-gated RevCAR T cells. *Front Immunol.* 2023;14:1166169.
23. Koristka S, Cartellieri M, Arndt C, et al. Retargeting of regulatory T cells to surface-inducible autoantigen La/SS-B. *J Autoimmun.* 2013;42:105-116.
24. Bachmann M, Troster H, Bartsch H, Grolz D. A frame shift mutation in a hot spot region of the nuclear autoantigen La (SS-B). *J Autoimmun.* 1996;9(6):747-756.
25. Bachmann MP, Bartsch T, Bippes CC, et al. T Cell mediated conversion of a non-anti-la reactive b cell to an autoreactive anti-la b cell by somatic hypermutation. *Int J Mol Sci.* 2021;22(3):1198.
26. Koristka S, Ziller-Walter P, Bergmann R, et al. Anti-CAR-engineered T cells for epitope-based elimination of autologous CAR T cells. *Cancer Immunol Immunother.* 2019;68(9):1401-1415.
27. Fasslrunner F, Arndt C, Koristka S, et al. Midostaurin abrogates CD33-directed UniCAR and CD33-CD3 bispecific antibody therapy in acute myeloid leukaemia. *Br J Haematol.* 2019;186(5):735-740.

28. Koristka S, Kegler A, Bergmann R, et al. Engrafting human regulatory T cells with a flexible modular chimeric antigen receptor technology. *J Autoimmun.* 2018;90:116-131.
29. Saleh HA, Mitwasi N, L RL, et al. RevCAR-expressing immune effector cells for targeting of Fn14-positive glioblastoma. *Cancer Gene Ther.* 2024;31(9):1323-1334.
30. Luken BM, Turenhout EA, Hulstein JJ, et al. The spacer domain of ADAMTS13 contains a major binding site for antibodies in patients with thrombotic thrombocytopenic purpura. *Thromb Haemost.* 2005;93(2):267-274.
31. Feys HB, Anderson PJ, Vanhoorelbeke K, Majerus EM, Sadler JE. Multi-step binding of ADAMTS-13 to von Willebrand factor. *J Thromb Haemost.* 2009;7(12):2088-2095.
32. Schelpe AS, Petri A, Roose E, et al. Antibodies that conformationally activate ADAMTS13 allosterically enhance metalloprotease domain function. *Blood Adv.* 2020;4(6):1072-1080.
33. Muia J, Zhu J, Gupta G, et al. Allosteric activation of ADAMTS13 by von Willebrand factor. *Proc Natl Acad Sci U S A.* 2014;111(52):18584-18589.
34. Schelpe AS, Roose E, Joly BS, et al. Generation of anti-idiotypic antibodies to detect anti-spacer antibody idiotopes in acute thrombotic thrombocytopenic purpura patients. *Haematologica.* 2019;104(6):1268-1276.
35. Pos W, Luken BM, Kremer Hovinga JA, et al. VH1-69 germline encoded antibodies directed towards ADAMTS13 in patients with acquired thrombotic thrombocytopenic purpura. *J Thromb Haemost.* 2009 Mar;7(3):421-428.
36. Postmus T, Schilder N, Ferreira de Santana J, et al. N-glycan shielded CUB domains of ADAMTS13 prevent binding of C-terminal antibodies in patients with immune-mediated TTP. *Blood Adv.* 2025;9(7):1728-1737.
37. Ostertag EM, Kacir S, Thiboutot M, et al. ADAMTS13 autoantibodies cloned from patients with acquired thrombotic thrombocytopenic purpura: 1. Structural and functional characterization in vitro. *Transfusion.* 2016;56(7):1763-1774.
38. Ferapontov A, Omer M, Baudrexel I, et al. Antigen footprint governs activation of the B cell receptor. *Nat Commun.* 2023;14(1):976.
39. Yang J, Reth M. Receptor Dissociation and B-Cell Activation. *Curr Top Microbiol Immunol.* 2016;393:27-43.
40. Schaller M, Vogel M, Kentouche K, Lammle B, Kremer Hovinga JA. The splenic autoimmune response to ADAMTS13 in thrombotic thrombocytopenic purpura contains recurrent antigen-binding CDR3 motifs. *Blood.* 2014;124(23):3469-3479.



41. Pos W, Sorvillo N, Fijnheer R, et al. Residues Arg568 and Phe592 contribute to an antigenic surface for anti-ADAMTS13 antibodies in the spacer domain. *Haematologica*. 2011;96(11):1670-1677.
42. Doyle AJ, Stubbs MJ, Dutt T, et al. Long-term risk of relapse in immune-mediated thrombotic thrombocytopenic purpura and the role of anti-CD20 therapy. *Blood*. 2023;141(3):285-294.
43. Selvakumar S, Liu A, Chaturvedi S. Immune thrombotic thrombocytopenic purpura: Spotlight on long-term outcomes and survivorship. *Front Med (Lausanne)*. 2023;10:1137019.
44. Ferrari S, Scheiflinger F, Rieger M, et al. Prognostic value of anti-ADAMTS 13 antibody features (Ig isotype, titer, and inhibitory effect) in a cohort of 35 adult French patients undergoing a first episode of thrombotic microangiopathy with undetectable ADAMTS 13 activity. *Blood*. 2007;109(7):2815-2822.
45. Muller F, Atreya R, Volkl S, et al. CD19 CAR T-Cell therapy in multidrug-resistant ulcerative colitis. *N Engl J Med*. 2025;393(12):1239-1241.
46. Wang X, Wu X, Tan B, et al. Allogeneic CD19-targeted CAR-T therapy in patients with severe myositis and systemic sclerosis. *Cell*. 2024;187(18):4890-4904.e9.
47. de Taeye SW, Bentlage AEH, Mebius MM, et al. FcγR binding and ADCC activity of human IgG allotypes. *Front Immunol*. 2020;11:740.
48. Sinkovits G, Szilagyi A, Farkas P, et al. Concentration and subclass distribution of anti-adamts13 igg autoantibodies in different stages of acquired idiopathic thrombotic thrombocytopenic purpura. *Front Immunol*. 2018;9:1646.
49. Ferrari S, Mudde GC, Rieger M, et al. IgG subclass distribution of anti-ADAMTS13 antibodies in patients with acquired thrombotic thrombocytopenic purpura. *J Thromb Haemost*. 2009;7(10):1703-1710.
50. Wermke M, Metzelder S, Kraus S, et al. Updated results from a phase I dose escalation study of the rapidly-switchable universal CAR-T therapy UniCAR-T-CD123 in relapsed/refractory AML. *Blood*. 2023;142(Supplement 1):3465.
51. Wermke M, Kraus S, Ehninger A, et al. Proof of concept for a rapidly switchable universal CAR-T platform with UniCAR-T-CD123 in relapsed/refractory AML. *Blood*. 2021;137(22):3145-3148.
52. Valitutti S, Muller S, Salio M, Lanzavecchia A. Degradation of T cell receptor (TCR)-CD3-zeta complexes after antigenic stimulation. *J Exp Med*. 1997;185(10):1859-1864.
53. Ellerman D. Bispecific T-cell engagers: Towards understanding variables influencing the in vitro potency and tumor selectivity and their modulation to enhance their efficacy and safety. *Methods*. 2019;154:102-117.

## **Figure Legends:**

**Figure 1: Reverse Chimeric Antigen Receptor (RevCAR T) cell production and Reverse Target Modules (RevTM) binding capacity.** **A.** RevCAR T-cell redirection strategy with the four candidate RevTMs to the right. **B.** (Left) RevCAR T cell transduction efficiency as assessed via the reporter marker Enhanced Green Fluorescent Protein (EGFP) (green) overlaid with untransduced control (grey). (Right) Average % EGFP of all donor T cells used in the assays. **C.** (Left) RevCAR staining to visualise correlation of RevCAR expression with EGFP. RevCAR-positive histogram peak (red), untransduced control (grey). (Right) Quantification of RevCAR expression as receptor density per T cell. **D.** RevTM binding assessment to RevCARs. **E.** RevTM binding to target hybridomas ( $\alpha$ -S, top and  $\alpha$ -CUB, bottom). **F, G.** RevTM binding to target Nalm-6 cells expressing patient-derived IL-1 ( $\alpha$ -S) (**F**) and z1-201 ( $\alpha$ -CUB) (**G**) scFvs. Overlaid histograms are shown. RMFI: Relative Median Fluorescence Intensity (RMFI) was calculated by subtracting the MFI of the secondary Ab control from the MFI of the stained sample

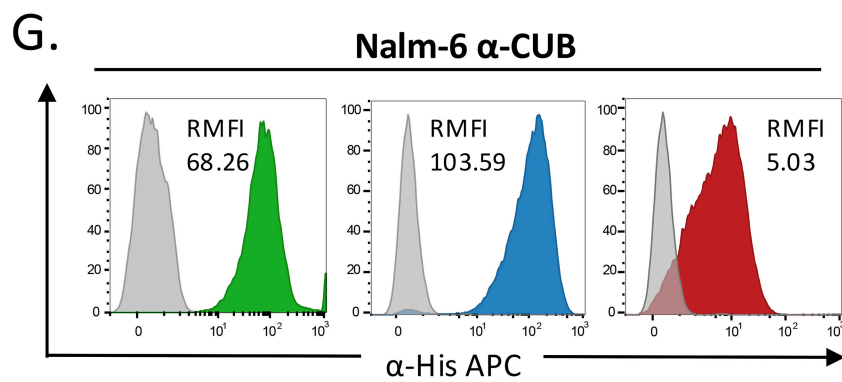
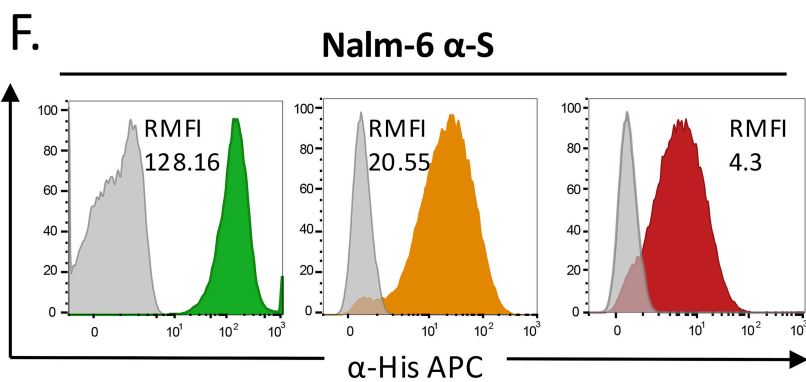
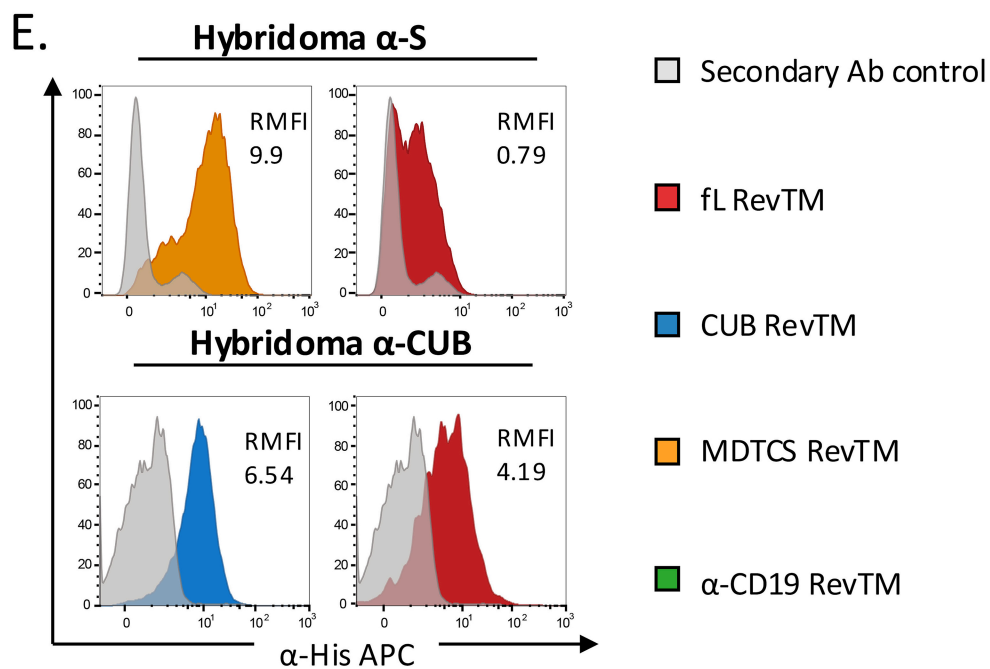
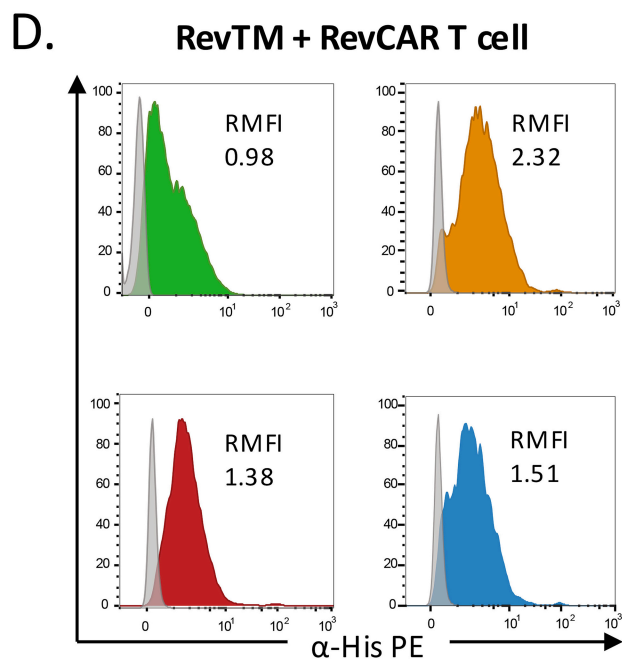
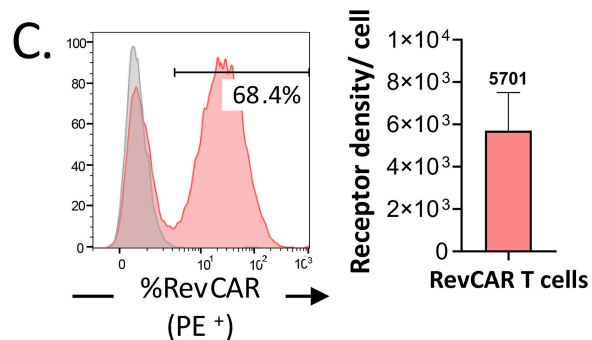
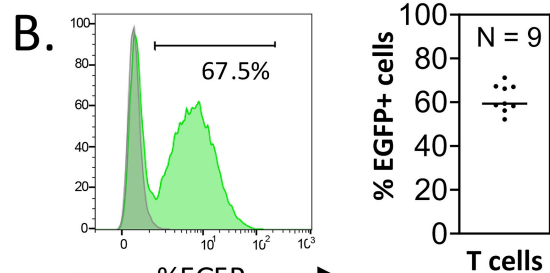
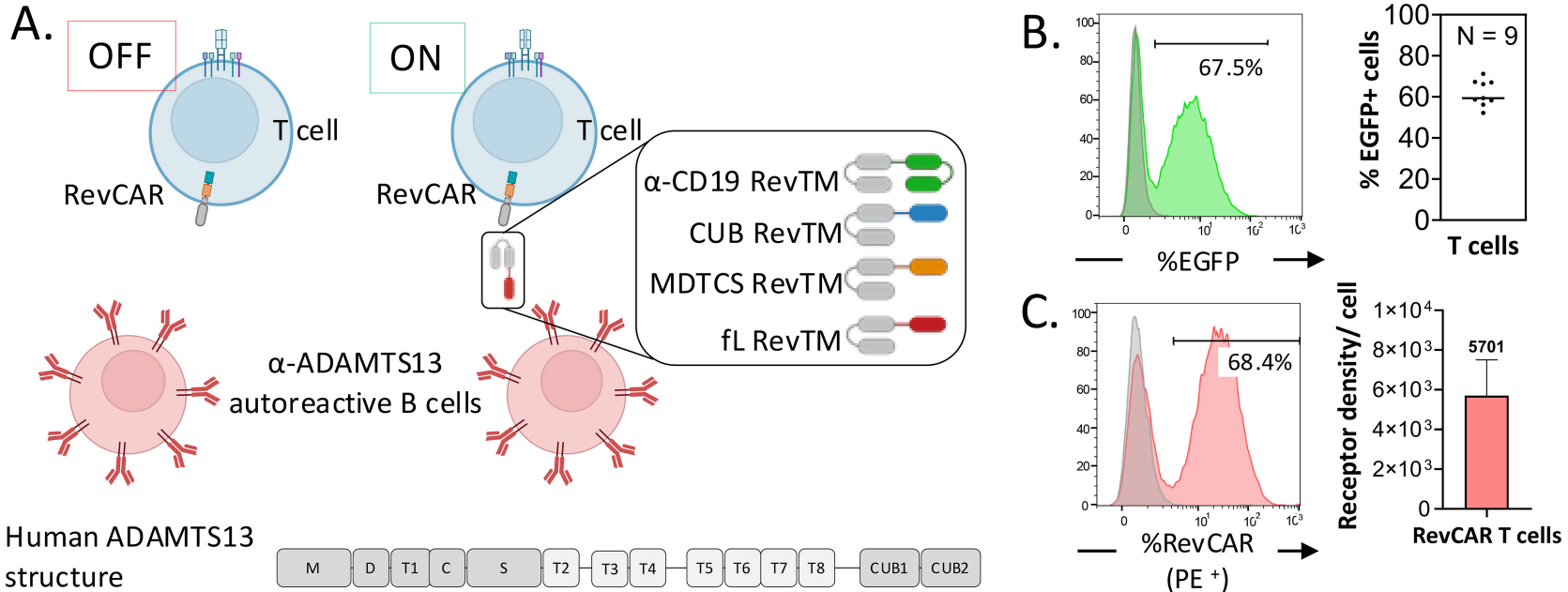
**Figure 2: RevTMs activate RevCAR T cells specifically and in a concentration-dependent manner against different target cells.** RevTM redirection efficiency against Nalm-6  $\alpha$ -S- and  $\alpha$ -CUB-expressing cells (**A**) and  $\alpha$ -S and  $\alpha$ -CUB hybridomas (**B, C**) at different RevTM concentrations. Co-cultures were setup at E:T ratios of 2.5:1 by staining target cells with eFluor 670 and incubating with RevCAR T cells and RevTMs. Co-cultures were analysed by assessing the target cell number via flow cytometry after 24 hours of co-incubation. Non-linear regression curve fit model was used to generate the EC<sub>50</sub> curve and interpolate the EC<sub>50</sub> value. Mean with SEM error bars are represented.

**Figure 3: RevCAR T cells retain cytotoxic ability even at low E:T ratios.** Co-culture assays were setup by staining the Nalm-6 (**A, B**) and Hybridoma (**C, D**) target cells with eFluor 670 and adding RevCAR T cells and RevTMs at a saturated concentration (25 nM for CUB and MDTCS RevTMs and 5 nM for  $\alpha$ -CD19 and fL RevTMs). Percentage lysis was read out after 24 hours of co-culture. Data was generated from independent experiments using T cells isolated from 3 donors. Paired t test, one-tailed; \*P  $\leq$  0.05; \*\*P < 0.001; \*\*\*P < 0.005 was performed by comparing all conditions with the respective condition without TM. Mean with SEM error bars are represented. P values are mentioned on top of each bar where the values are non-significant.

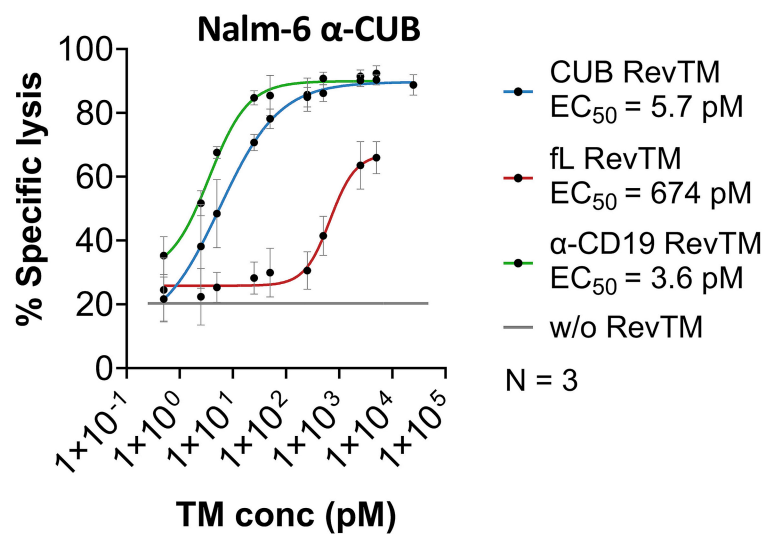
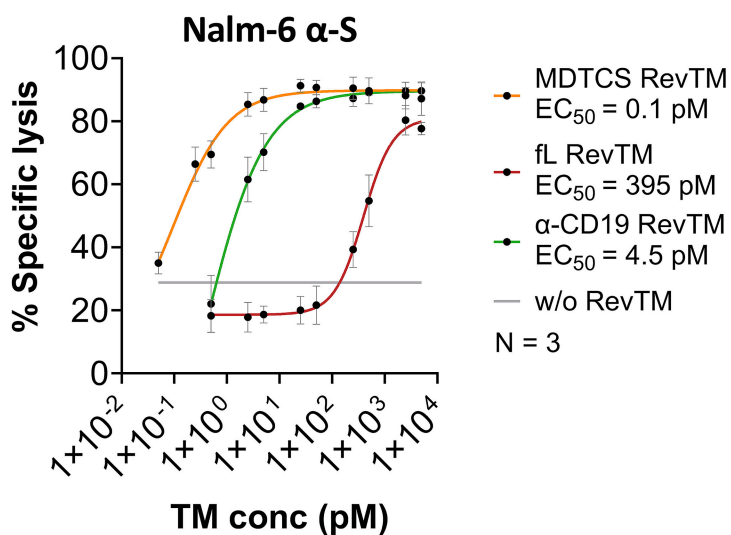
**Figure 4: RevTMs specifically stimulate RevCAR T cells to secrete various cytokines.** Sandwich Enzyme-linked Immunosorbent Assay (ELISA) was performed on the co-culture supernatants to quantify different proinflammatory and proliferative cytokines like Interleukin -2 (IL-2), Tumor Necrosis Factor (TNF), Interferon gamma (IFN- $\gamma$ ) and Granulocyte Monocyte Colony Stimulating Factor (GM-CSF). RevCAR T cells specifically release these cytokines only in the presence of the respective RevTM and target Nalm-6 (**A, B**) and hybridoma cells (**C, D**), albeit at different levels. Data was generated from independent experiments using T cells isolated from 3 donors. Paired t test, one-tailed; \*P  $\leq$  0.05; \*\*P < 0.001; \*\*\*P < 0.005 was performed by comparing all conditions with the respective condition without TM. Mean with SEM error bars are represented. P values are mentioned on top of each bar where the values are non-significant.

**Figure 5: RevTMs specifically stimulate RevCAR T cells to express cytotoxic effector molecules.** RevCAR T cells were stained intracellularly for Granzyme B and Perforin 24 hours after co-culture. Effector molecules were analysed in both CD8-positive and negative RevCAR T cells in co-cultures against Nalm-6  $\alpha$ -S (**A, B**), Nalm-6  $\alpha$ -CUB (**C, D**), Hybridoma  $\alpha$ -S (**E, F**) and Hybridoma  $\alpha$ -CUB (**G, H**). Raw data histogram plots for one representative donor showed on the left of each sub-panel. Data was generated from independent experiments using T cells isolated from 3 donors. Paired t test, one-tailed; \*P  $\leq$  0.05; \*\*P < 0.001; \*\*\*P < 0.005 was performed by comparing all conditions with the respective condition without TM. P values are mentioned on top of each bar where the values are non-significant.

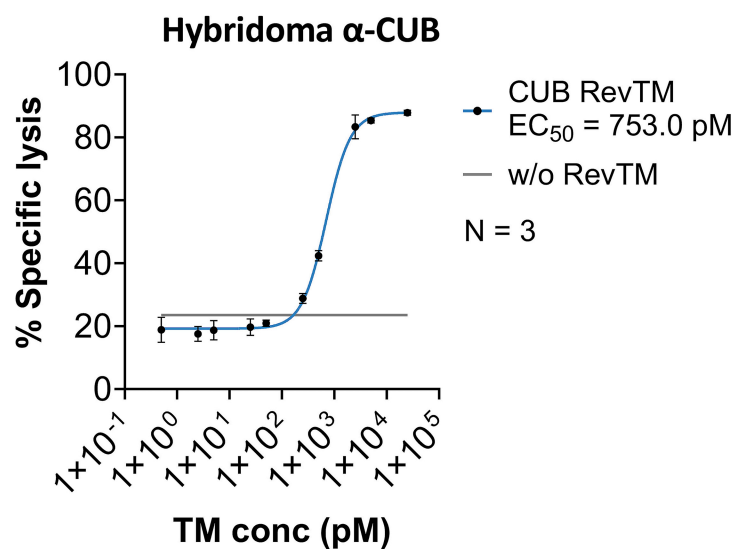
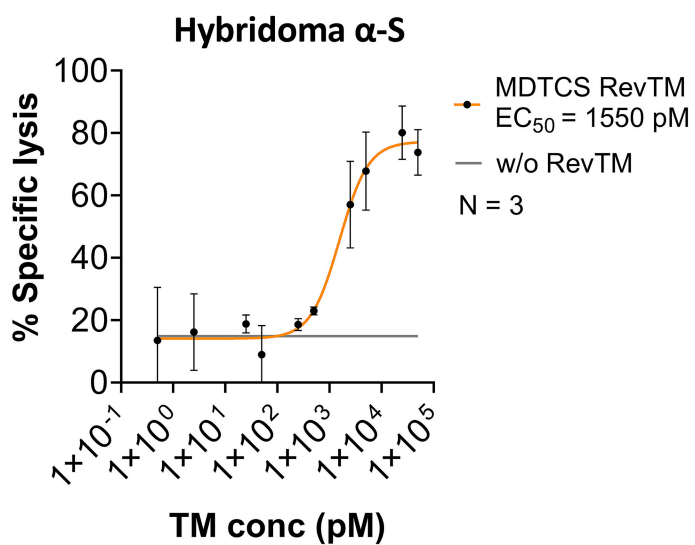
**Figure 6: RevCAR adaptor system retains cytotoxic ability even in the presence of high concentrations of autoantibodies.** Co-culture assay conditions: RevTM concentration – 25 nM, E:T ratio – 2.5:1, co-culture time – 24 hours and increasing concentrations of autoantibodies against both Nalm-6 (**A**) and hybridoma (**B**) target cell lines. Data was generated from independent experiments using T cells isolated from 3 donors. Statistical analysis was performed by comparing all conditions with condition without TM. Paired t test; two-tailed; \*P  $\leq$  0.05; \*\*P < 0.001; \*\*\*P < 0.005.



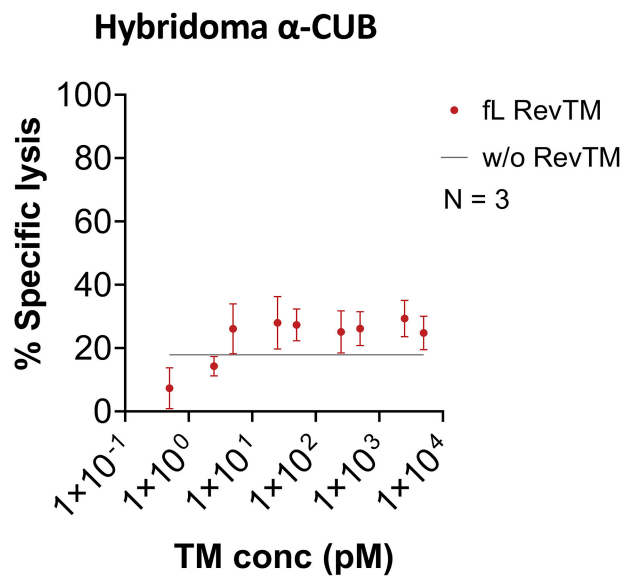
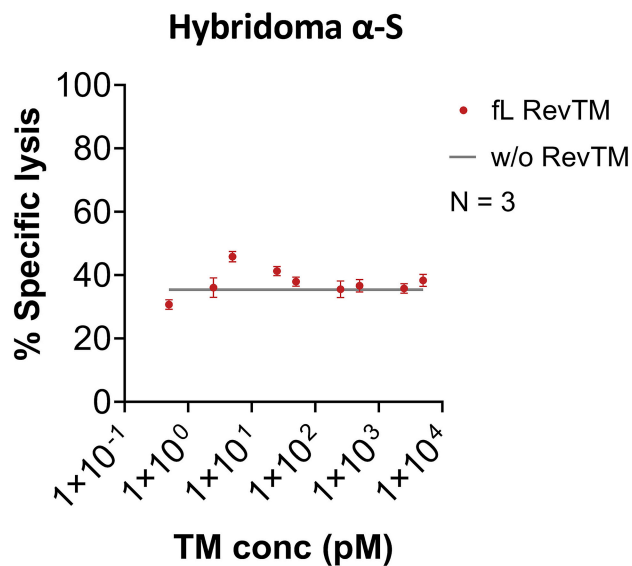
A.



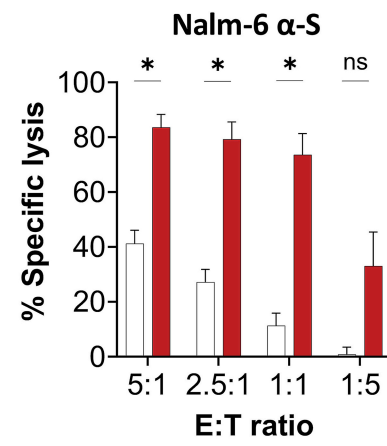
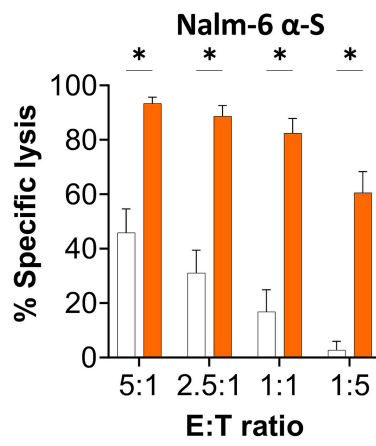
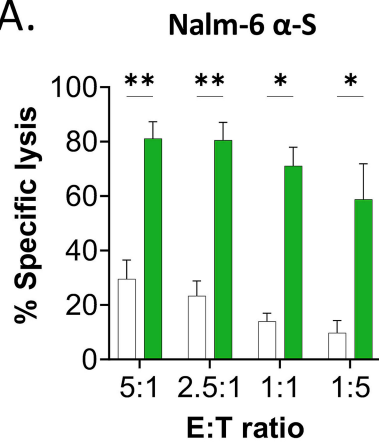
B.



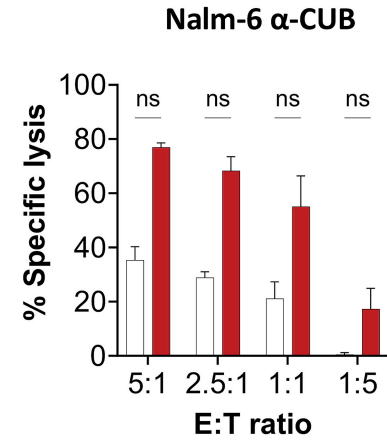
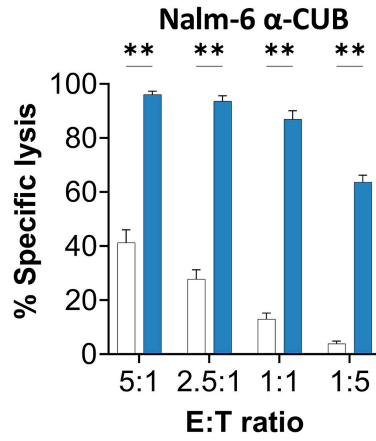
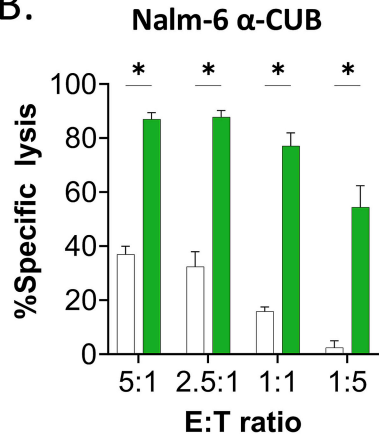
C.



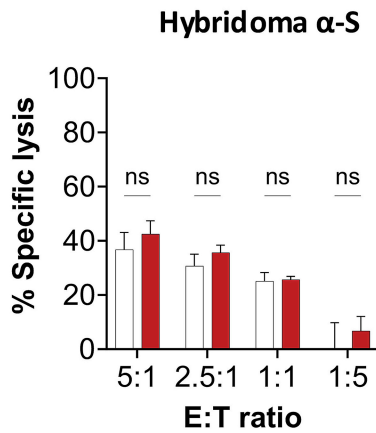
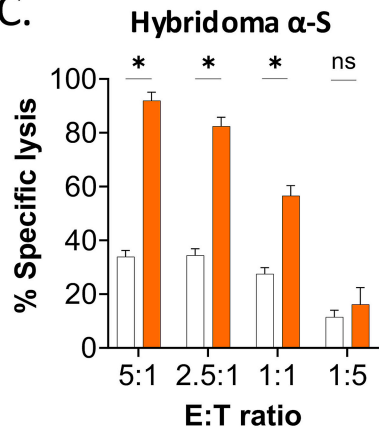
A.



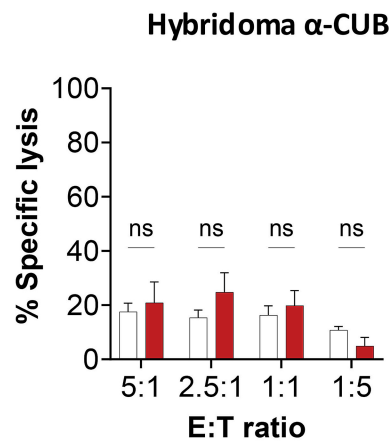
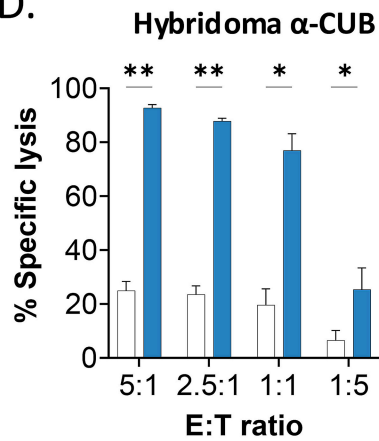
B.



C.



D.



□ w/o RevTM

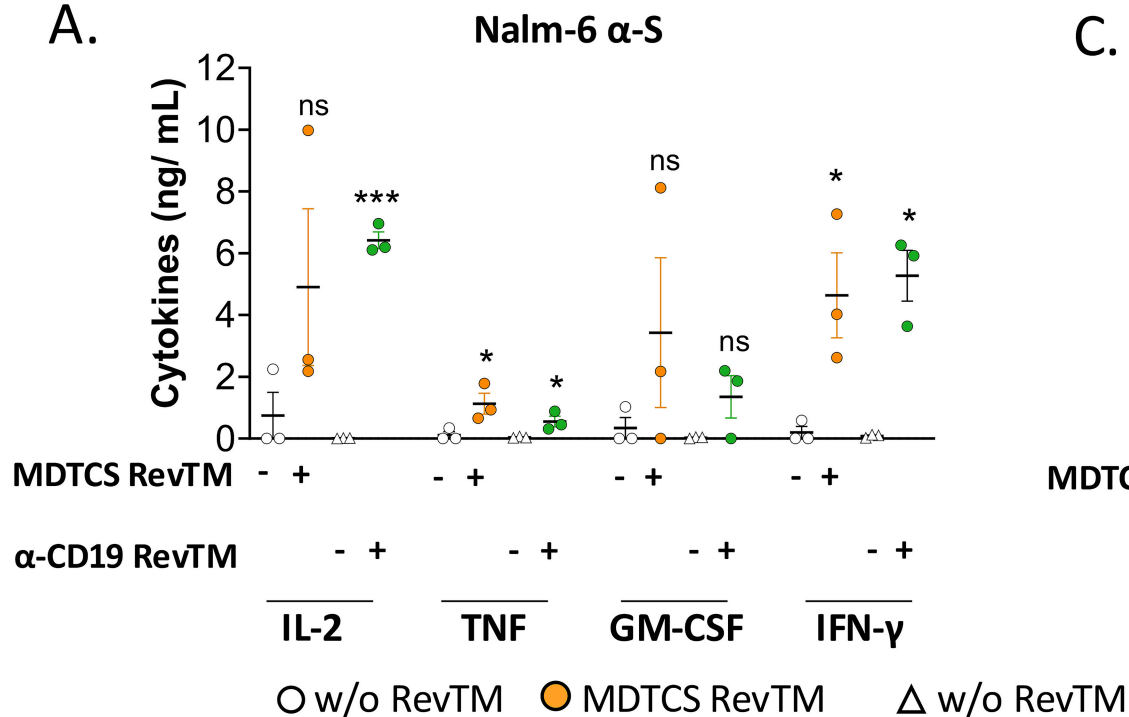
■  $\alpha$ -CD19 RevTM

■ MDTCS RevTM

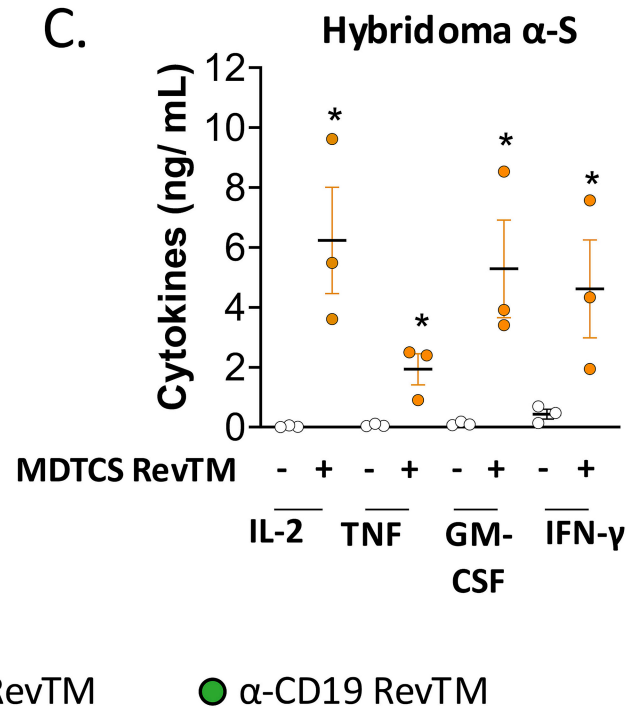
■ fL RevTM

■ CUB RevTM

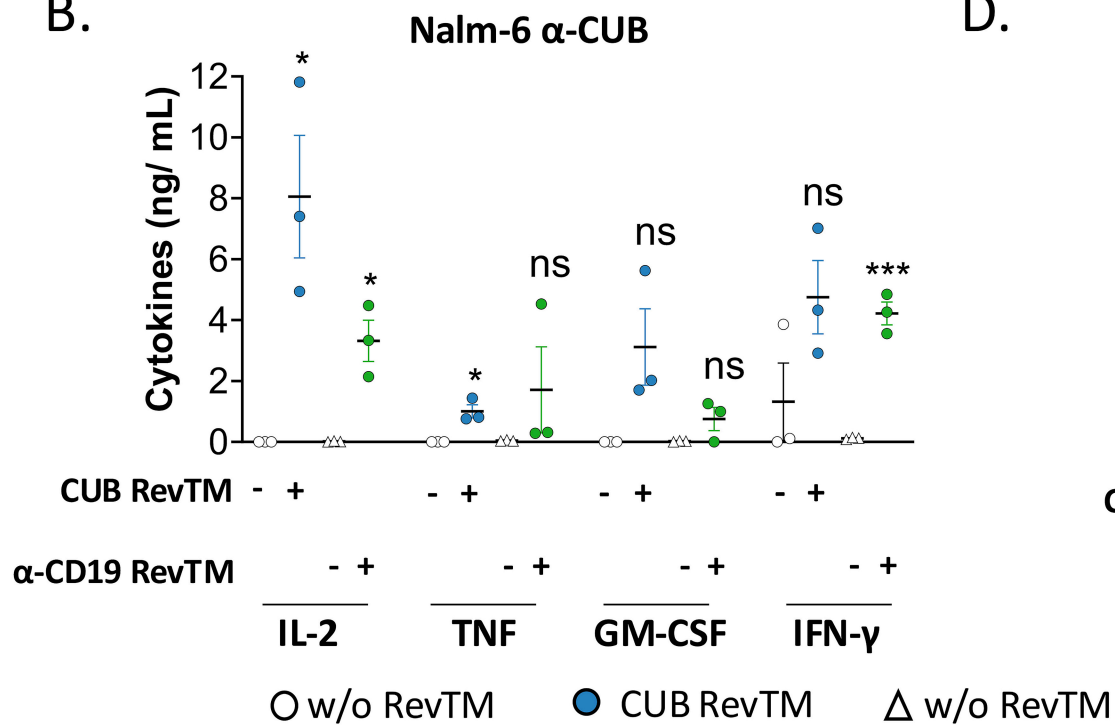
A.



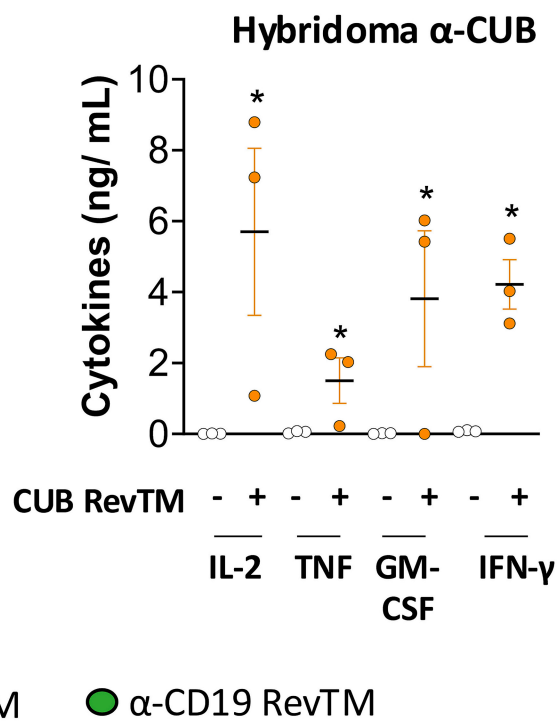
C.

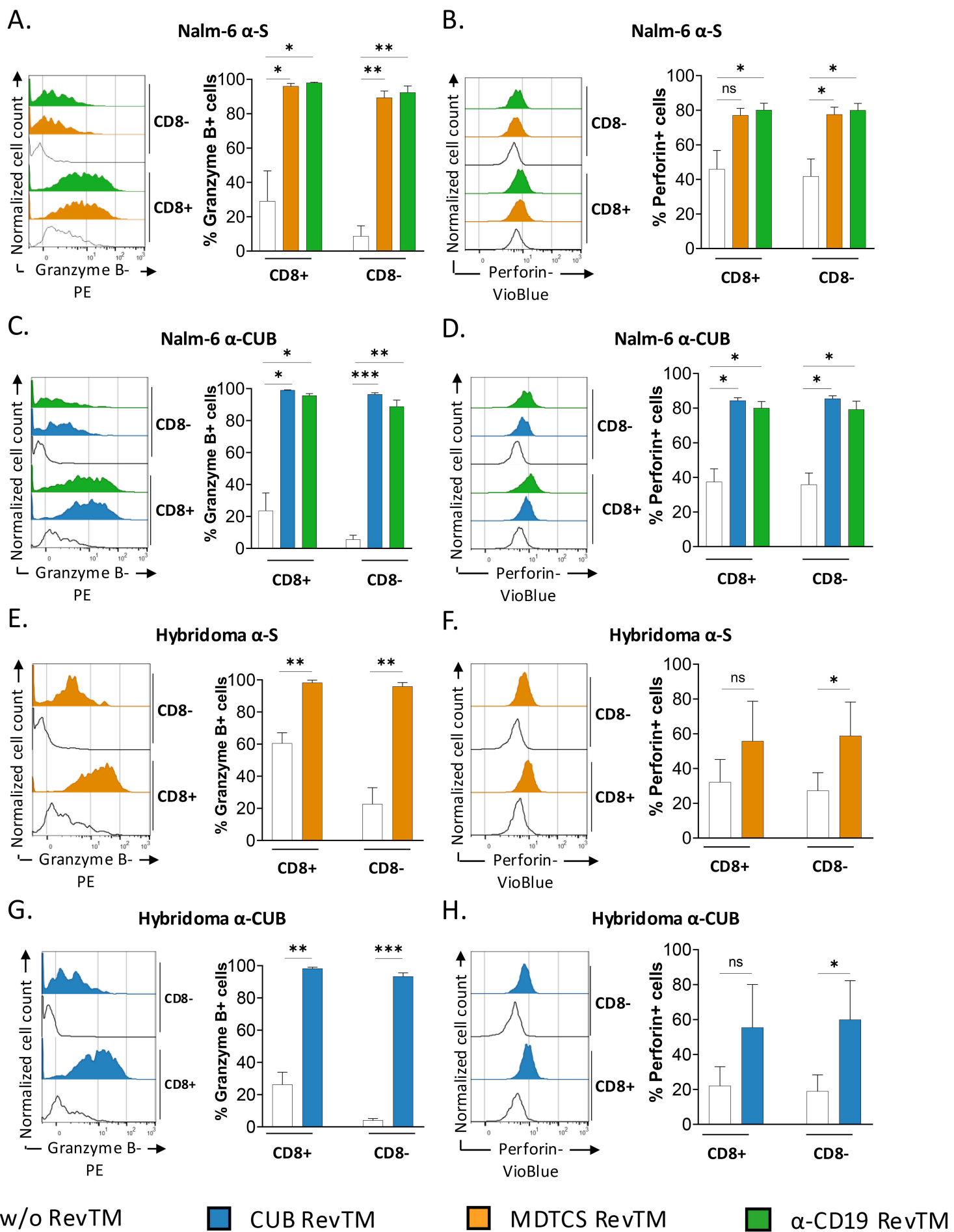


B.

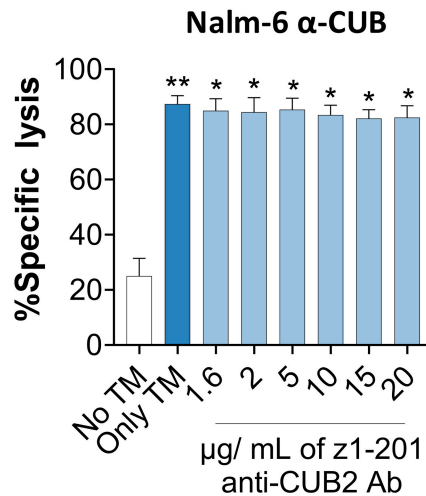
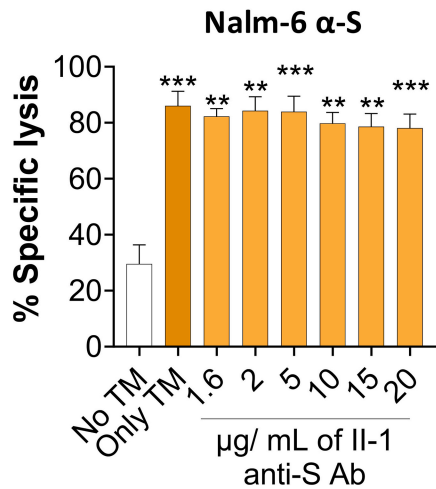


D.

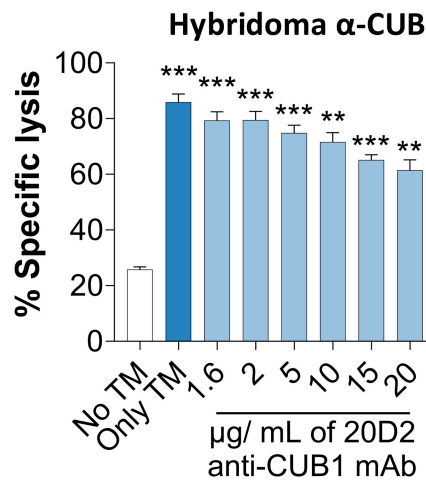
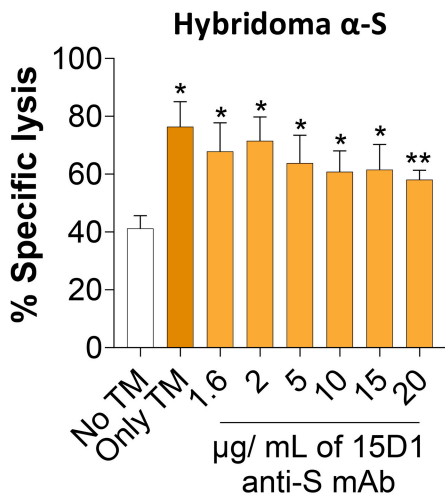




A.



B.



□ w/o TM

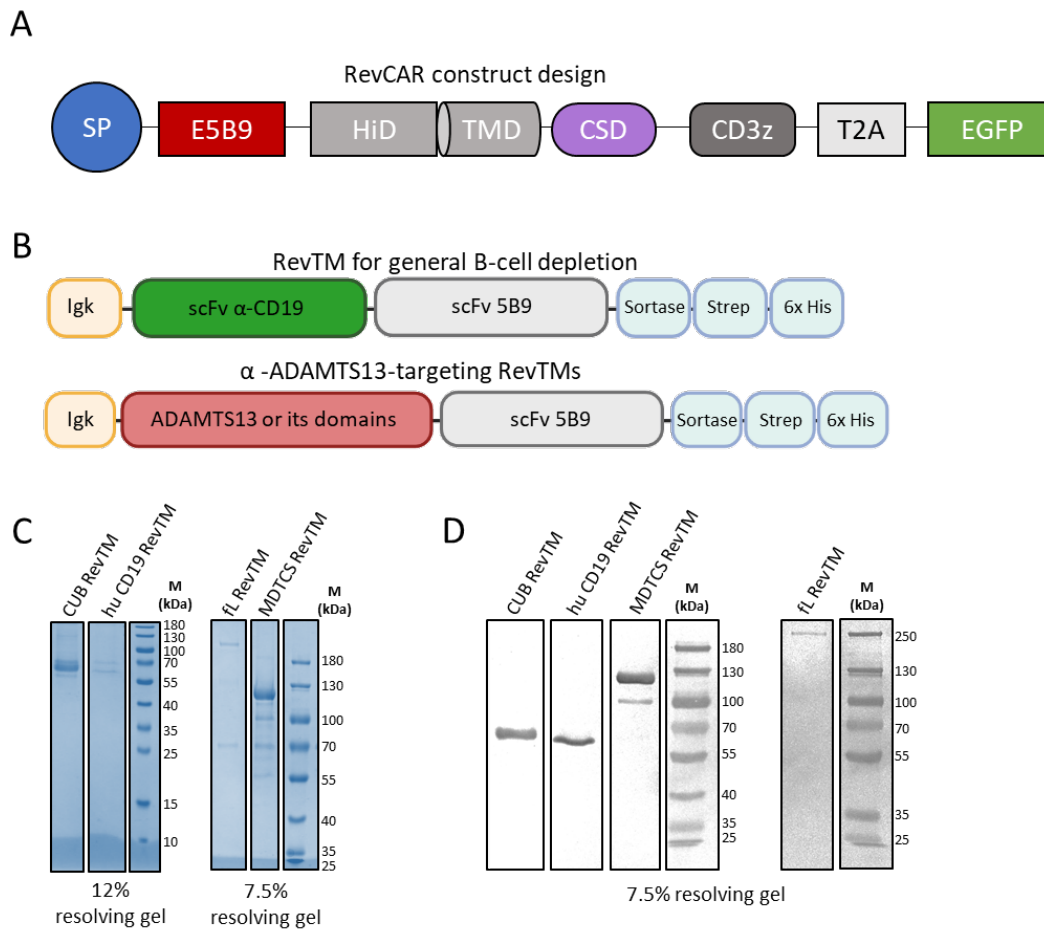
■ CUB RevTM +  
 $\alpha$ -CUB1 mAb

■ MDTCS RevTM

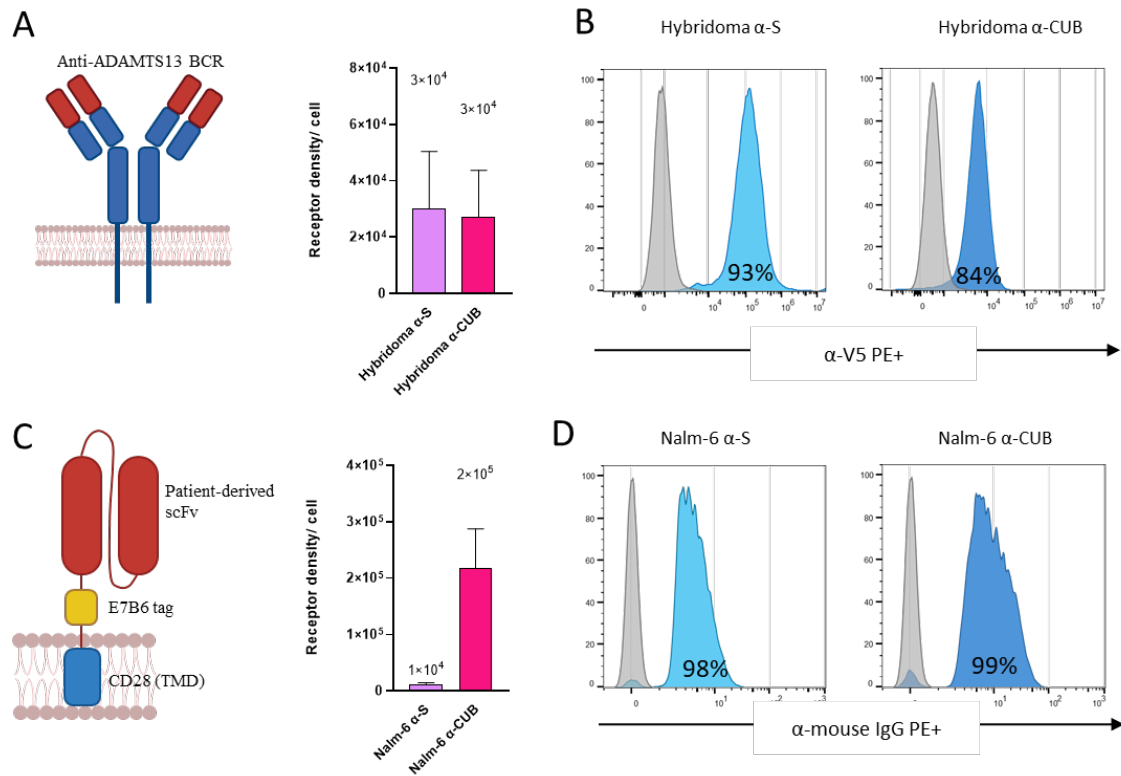
■ CUB RevTM

■ MDTCS RevTM +  
 $\alpha$ -S mAb



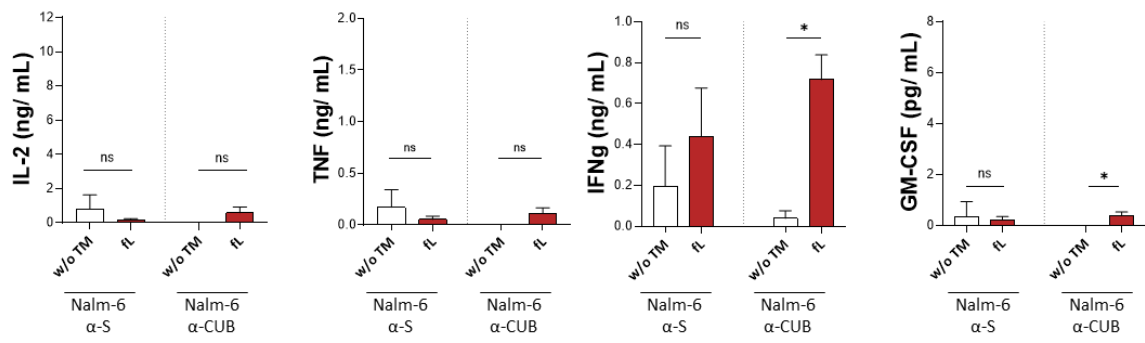
**Supplementary material:**

**Supplementary Figure S1:** (A) RevCAR construct design; SP: Signal peptide, HiD: Hinge domain, TMD: transmembrane domain, CSD: co-stimulatory domain, CD3: CD3 zeta, T2A: self-cleaving peptide sequence, EGFP: Enhanced green fluorescence protein. (B) Structure of RevTM targeting both  $\alpha$ -ADAMTS13 autoreactive B cells and hu CD19. (B) Coomassie-stained SDS gel with purified CUB, MDTCS, ADAMTS13 and  $\alpha$ -hu CD19 RevTMs. (C) Western blots with purified CUB, MDTCS, ADAMTS13 and  $\alpha$ -hu CD19 RevTMs developed using  $\alpha$ -His IgG + rabbit- $\alpha$ -mouse IgG Alkaline phosphatase. Each panel containing gel images was grouped from the same gel and paired with its corresponding marker. For panel D, non-linear adjustment using the gamma-contrast were made.

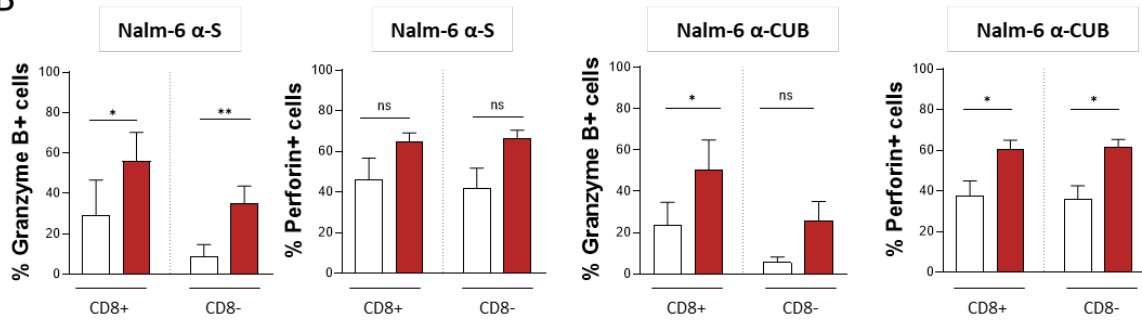


**Supplementary Figure S2:** (A) Left, pictorial representation of  $\alpha$ -S/  $\alpha$ -CUB1 receptor on hybridomas; right, receptor density/ cell of each hybridoma used. (B)  $\alpha$ -S (left) and  $\alpha$ -CUB1 (right) BCR expression as confirmed by flow cytometry staining of  $\alpha$ -S and  $\alpha$ -CUB hybridomas respectively. (C) Left, pictorial representation of  $\alpha$ -S/  $\alpha$ -CUB2 receptor on Nalm-6 cells; right. Patient-derived scFv (II-1:  $\alpha$ -S, or z1-201:  $\alpha$ -CUB) and La-derived E7B6 epitope on the extracellular part while CD28-derived transmembrane domain (TMD) for anchoring. Receptor density/ cell of each Nalm-6 cell line used. (D)  $\alpha$ -S (left) and  $\alpha$ -CUB (right) decoy receptor expression as confirmed by flowcytometry staining of Nalm-6  $\alpha$ -S and  $\alpha$ -CUB respectively. Receptor density quantification done in three independent experiments. SEM represented.

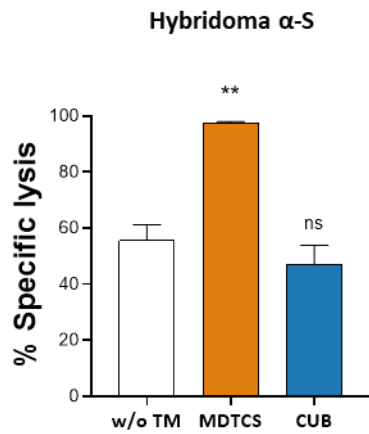
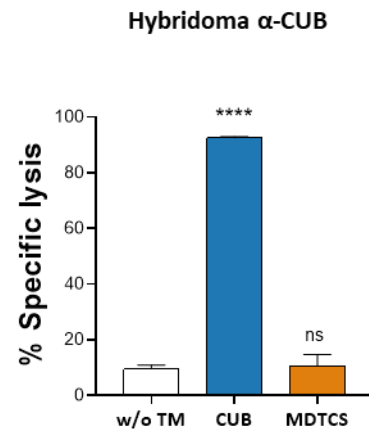
A



B



**Supplementary Figure S3:** Cytokine secretion (A) and granzyme and perforin expression (B) profile of RevCAR T cells when co-cultured with fL RevTM and corresponding target Nalm-6 cells. Data generated using T cells isolated from 3 donors. Paired t test, one-tailed; \*P < 0.05; \*\*P < 0.001; \*\*\*P < 0.005, \*\*\*\*P < 0.0005 was performed by comparing all conditions with the respective condition without TM.

**A****B**

**Supplementary Figure S4:** RevTMs specifically redirect RevCAR T cells to kill target cells. In vitro co-culture assay between RevCAR T cells and  $\alpha$ -S (A) or  $\alpha$ -CUB (B) hybridomas. RevCAR T cells were co-cultured with hybridomas at 2.5:1 E:T ratio and 25 nM RevTM. Number of target cells were enumerated on flow cytometer 24 hours after co-culture. Data generated for T cells isolated from 3 healthy donors. Paired t test, two-tailed; \* $P < 0.05$ ; \*\* $P < 0.001$ ; \*\*\* $P < 0.005$ , \*\*\*\* $P < 0.0005$  was performed by comparing all conditions with the respective condition without TM.

## **Supplementary Methods:**

### **Cell culture**

Hybridoma and Nalm-6 were the two target cell lines used for characterization and functional validation of the RevCAR system. In-house (KU Leuven) hybridoma 15D1 expressed the  $\alpha$ -S BCR and 20D2 the  $\alpha$ -CUB1 BCR<sup>1,2</sup>. These cells were cultured in DMEM medium supplemented with 10% bovine serum optimized for hybridomas (GE Healthcare), 1% MEM Non-Essential Amino Acids (NEA) solution (Invitrogen), 0.0004%  $\beta$ -Mercaptoethanol (Sigma Aldrich), 1% Penicillin-Streptomycin (Invitrogen), 2% HT-supplement (Invitrogen), 20 mM HEPES (Invitrogen). Nalm-6 cells were engineered to express a patient-derived  $\alpha$ -S (II-1) and  $\alpha$ -CUB2 (z1-201) single-chain fragment variable (scFv) on their surface via lentiviral transduction and were cultured in RPMI medium supplemented with 10% Fetal Calf Serum (FCS), 1% Penicillin-Streptomycin, 1% MEM NEA, 1% L-Alanine-L-Glutamine, 1% Sodium pyruvate (RPMI complete). Murine fibroblast 3T3 cells and HEK293T cells were cultured using DMEM medium supplemented with 10% FCS, 1% Pen-Strep, 1% MEM NEA (DMEM complete). All cells were maintained at 37 °C and 5% CO<sub>2</sub>.

### **Construction, expression and quantification of recombinant RevTMs**

For construction of the pan B cell depleting  $\alpha$ -CD19 RevTM, the  $\alpha$ -human CD19 scFv (monoclonal antibody (mAb) clone HD-37) was fused with the  $\alpha$ -La scFv (5B9) (Figure 1A). RevTMs targeting  $\alpha$ -ADAMTS13 B cells were generated by linking full-length (fL) ADAMTS13, MDTCS or CUB1-2 domains to the  $\alpha$ -La scFv (5B9) to form the fL, MDTCS and CUB RevTMs respectively. All RevTMs were equipped with C-terminal Strep and 6x His tags to aid protein purification (Figure 1A). Moreover, the murine Ig kappa leader was added as a signal peptide (SP) to the N-terminus of all RevTMs to enable their secretion in the cell culture supernatants (Supplementary Figure S1A).

For generation of persistent RevTM-producing 3T3s,  $0.75 \times 10^6$  HEK293T cells were cultured in 90 mm cell culture dish (Greiner Bio-One) on day 0. On day 3, the cloned RevTM plasmids, along with packaging plasmids, were co-transfected in HEK293T cells as described<sup>3</sup>. The supernatant of the transfected HEK cells was then collected four times, every 12 hours, filtered and transferred onto 3T3 cells at each timepoint, and fresh DMEM complete medium was added onto HEK293T cells. After four transductions, the HEK293T cells were discarded, and the 3T3 cells were further treated with the selection antibiotic Zeocin at 0.3 mg/ mL concentration to enrich the transduced cells, until the enrichment was  $\sim 99\%$ . The transduction efficiency was monitored via the reporter gene EGFP in the TM construct by flow cytometry.

The purified RevTMs were analyzed by SDS-PAGE followed by Quick Coomassie staining<sup>4</sup> or Western blotting. For immunodetection, proteins were transferred to nitrocellulose and probed using anti-His mAb (Qiagen, 1:2500) and rabbit-anti-mouse IgG alkaline phosphatase (Biozol, 1:1000).

### **Binding assessment using flow cytometry**

Binding of the RevTMs to target cells (hybridoma and Nalm-6) and RevCAR T-cells was determined via flow cytometry. For this,  $2 \times 10^5$  cells were incubated with the respective

RevTM (20 µg/ml) for 1 h at 4 °C, washed with PBS/2% FCS, and then incubated again for 30 min at 4 °C with  $\alpha$ -His-PE (1:50) or  $\alpha$ -His APC (1:100) mAb (Miltenyi Biotec). Shortly before analysis, cells were counterstained with propidium iodide to allow for live-dead-cell discrimination. The stained cells were measured with the MACSQuant10 Analyzer (Miltenyi Biotec), and the results were analyzed with MACSQuantify (Miltenyi Biotec) or FlowJo™ Software.

Surface expression of  $\alpha$ -S BCR/scFv,  $\alpha$ -CUB BCR/scFv and RevCARs on target or effector cells was determined in a similar way. For detection of  $\alpha$ -S scFv and  $\alpha$ -CUB scFv on Nalm-6, cells were stained with 20 µg/ml  $\alpha$ -La 7B6 mAb (in-house) as primary antibody and goat  $\alpha$ -mouse PE mAb (Invitrogen, 1:50) as the secondary antibody. RevCAR expression was detected by using first 20 µg/ml  $\alpha$ -La 5B9 mAb (Davids) and second goat  $\alpha$ -mouse PE mAb (Invitrogen, 1:50). As negative control, cells were only stained with the secondary mAb in combination with the corresponding isotype control antibody (7B6: mouse IgG1,  $\kappa$ ; 5B9: mouse IgG2b,  $\kappa$  (Biolegend). For detection of  $\alpha$ -S or  $\alpha$ -CUB BCRs on hybridomas, cells were incubated with MDTCS-V5 or T2-C2-V5 respectively and then stained with  $\alpha$ -V5 PE mAb (eBioscience). To determine antigen density on the cell surface, the Quantitative Analysis Kit QIFIKIT® (Agilent) was used following the manufacturer's instructions. Data was plotted using GraphPad prism 10 software.

1. Fasslrinner F, Arndt C, Koristka S, et al. Midostaurin abrogates CD33-directed UniCAR and CD33-CD3 bispecific antibody therapy in acute myeloid leukaemia. *Br J Haematol*. Sep 2019;186(5):735-740. doi:10.1111/bjh.15975
2. Koristka S, Ziller-Walter P, Bergmann R, et al. Anti-CAR-engineered T cells for epitope-based elimination of autologous CAR T cells. *Cancer Immunol Immunother*. Sep 2019;68(9):1401-1415. doi:10.1007/s00262-019-02376-y
3. Loff S, Dietrich J, Meyer JE, et al. Rapidly Switchable Universal CAR-T Cells for Treatment of CD123-Positive Leukemia. *Mol Ther Oncolytics*. Jun 26 2020;17:408-420. doi:10.1016/j.omto.2020.04.009
4. Koristka S, Cartellieri M, Theil A, et al. Retargeting of human regulatory T cells by single-chain bispecific antibodies. *J Immunol*. Feb 1 2012;188(3):1551-8. doi:10.4049/jimmunol.1101760